Universita' degli Studi di Napoli "Federico II"

RESEARCH DOCTORATE
in
COMPUTATIONAL BIOLOGY and BIOINFORMATICS
XXV CYCLE

miRNA and proteins in Neuroblastoma tumorigenesis: perspectives analyses on miR34a function

PhD Student: Marianeve Carotenuto

Tutor: Prof. Massimo Zollo

Co-Tutor: Prof. Giovanni Paolella

Table of contents

Abstract

Neuroblastoma is a childhood cancer that originates from precursor cell of sympathetic nervous system, occurring primarily in children under the age of 5 years. The disease is highly heterogeneous, ranging from spontaneous regression to rapid progression with high death rate in pediatric oncology. Expression profiling studies of Neuroblastoma primary tumors have identified many miRNAs whose expression levels have been significantly associated with poor patient survival. MiR-34a is a member of an evolutionarily conserved miRNA family, miR-34s. Mir34a functions as tumor suppressor in Neuroblastoma and the inactivation and absence of miR-34a has been shown related to the pathogenesis of a variety of tumors. Several genes have been shown to be direct miR-34a targets, encoding for proteins involved in proliferation, invasion and apoptosis. However, it is likely that miR-34a regulates many additional, as yet unconfirmed targets, since bioinformatic predictions suggest that several hundred of mRNAs contain matches to the miR-34a seed sequence. To address this question, here, we describe a global analysis of the effect of miR-34a expression at early time points (6 and 12 hrs) on proteome using a shotgun analysis with post-metabolic differential labeling in two different aggressive Neuroblastoma cell lines. This technology allow us to identify 2082 proteins, of which 172 were found differentially regulated, with 113 proteins being down- and 68 up-regulated. Computational analyses were employed to assign to each identified peptide its protein name and its specific level of regulation. When considering protein with a predicted seed-matching site among the protein identified, we found that only 33 proteins retain seed sequence in the 3' UTR of the corresponding mRNA, as predicted by PITA tool. By combining the results generated by shotgun and Kaplan Meier for overall survival analyses, we found seven proteins/genes correlated to worse clinical outcome when overexpressed in NBL. These genes are involved in the differentiation (LYAR, CTCF), apoptosis and proliferation (TGM2, Ki67), molecular transport (TIMM13 and ABCF2) and several

metabolic pathway (ALG13). Furthermore, these proteins are strongly linked each other and their impairment affects several pathways, including those signaling pathways such as TGF-β, Wnt and Src. Here, we comprehensively demonstrate the capabilities of miR-34a to target simultaneously components of several cancer signaling cascade, involved in Neuroblastoma progression. The level of this analysis was able to deeply understand which other protein are targeted and at what specific time of action are then down-regulated by miR34a, given a second level of target identification and showing the importance of this action in Neuroblastoma as one of the prominent phenomena occur to counteract the progression of tumorigenesis.

Moreover, we demonstrated that the magnitude of miR-34a effect on protein expression changes occurs at early time when compared to the later proteome output. Finally, to assess trend analysis, of the proteins differentially expressed at different time points (6h, 12h and 24h), Lorenz curve and Gini coefficient were evaluated for each protein, observing that several proteins were dinamically regulated and highlighting that machinery involving protein downregulation, by miRNA, are not linear. Our data along with previous studies strongly suggest the potential therapeutic usefulness of miR-34a that could offer better chance of therapeutic success.

Introduction 1

1. Introduction

1.1 Neuroblastoma

Neuroblastoma (NB) is the most common extra-cranial solid tumor of childhood. It has an incidence of 1 to 5 per million children per year and it is responsible for approximately 15% of all childhood cancer mortality. NBs originate from immature sympathetic nervous system cells, the so-called neuroblasts. Most NBs (90%) are diagnosed before the age of 5 years, and the median age of occurrence is approximately 22 months [1]. The vast majority of tumors arise sporadically, although some familial cases are described. Most of the tumors are found in the abdomen (65%), often in the adrenal medulla, or elsewhere in the human body where sympathetic nervous system components are present [2]. NBs belong to the subgroup of small round blue cell tumors and can often pose a challenge to the pathologist because of their similarities with lymphomas, rhabdomyosarcomas, the Ewing family of tumors and desmoplastic round cell tumors. NB tumors are divided into different stages according to the localization and extension of the primary tumor and the absence or presence of distant metastases. The International Neuroblastoma Risk Grouping Staging System takes into account the extent of disease at diagnosis as well as risk factors and stages defined using imaging to classify NBs from patients from all over the world in a uniform manner [3,4]. Metastatic tumors (stage M) have a dismal prognosis, whereas patients with locoregional tumors (L1 and L2) usually have an excellent outcome. Stage Ms tumors (where 's' stands for special and metastatic disease is confined to skin, liver and/or bone marrow) are characterized by spontaneous regression or differentiation even without any form of therapy. Although localized disease can be treated by surgery alone, the standard therapy for patients with metastatic disease usually comprises intensive induction chemotherapy, local surgery and myeloablative chemotherapy followed by autologous stem cell transplant, external radiotherapy and retinoic acid treatment. The overall survival rate for children with metastatic NB is approximately 40%, despite

this intensive multimodal therapy. The survival of children with NB also correlates strongly with age at diagnosis. Children under 1 year at diagnosis usually have a favorable prognosis, whereas prognosis of older children presenting with NB is poor.

Currently, there are worldwide efforts to construct a robust risk stratification system. Before any treatment, patients will be put into a risk category, according to a combination of parameters such as age (younger or older than 18 months), stage, pathology, MYCN status, other genetic aberrations such as 11q loss and ploidy [3,4]. The use of the International Neuroblastoma Risk Groups will allow international comparisons of different risk-based therapeutic approaches in the same patient population and greatly facilitate joint international collaborative studies in NB. Elucidation of the molecular pathways involved will enable researchers to stratify the disease and to adapt therapy.

1.2 Genomic analysis of Neuroblastoma

The clinically heterogeneous nature of NB depends, in part, by its biological and genetic heterogeneity. During the past decade, several genetic aberrations have been discovered in NB primary tumors and cell lines that have been shown to correlate with the various clinical features. Moreover, genetic and molecular findings are now routinely incorporated into therapeutic decision making [5]. The most important genetic defects that have been detected in NB are briefly discussed below.

**Ploidy** According to their DNA index, NBs can be divided into a group with a near-diploid nuclear DNA content (about 45% of NBs) and those with a near-triploid DNA content (about 55%). DNA index is a prognostic marker for patients younger than 2 years with disseminated disease [6-8]. It was suggested that a near-triploid DNA content, which is found more often in localized or Ms NB, was due to the fact that these tumors have a fundamental defect in mitosis leading to gains and losses of whole chromosomes, whereas locoregional or

metastatic tumors with a near diploid DNA content have a fundamental defect in genome stability leading to chromosomal rearrangements such as unbalanced translocations.

__MYCN amplification__ The MYCN oncogene was found to be amplified in 20 to 25% of NBs, and is usually present in the form of double-minutes (chromosome fragments) or homogeneously staining regions. Evidence for a direct involvement in the development of NB was obtained through the construction of a mouse NB model in which a human MYCN cDNA was placed under the control of a tyrosine hydroxylase promoter, leading to development of NB [9]. Amplification of the MYCN gene is most often found in high-stage tumors and is a marker for poor outcome [10,11].

Although MYCN regulates a large number of downstream genes, only a handful of key targets have yet been identified. Interestingly, high MYCN target gene expression is not restricted to MYCN-amplified NBs but is also apparent in high-stage MYCN non-amplified tumors, indicating that common pathways are altered in high-stage tumors [12].

__Chromosome 3p loss__ Chromosome 3p loss is often found in association with 11q loss and typically occurs in tumors without MYCN amplification or 1p deletion [13-16]. Furthermore, tumors with 3p loss are a hallmark of NB patients with older age at diagnosis, suggesting that 3p loss is a late event in NB oncogenesis. At present, three common regions of deletions on the short arm of chromosome 3 can be delineated [17]. Two of these SRDs were found to coincide with SRDs defined in more common cancers, such as breast and lung cancer [17]. These regions contain several candidate tumor suppressor genes, including the RASSF1A gene.

__Chromosome 11q loss__ Deletions of the long arm of chromosome 11 have been identified in 15 to 22% of primary NBs. Chromosome 11q deletions are often found in high-stage tumors without MYCN amplification and with intact chromosome 1p. Chromosome 11q loss was shown to be associated with reduced time of progression-free survival [18,19]. Recently, two common

regions of deletion on the long arm of chromosome 11 were delineated and CADM1 was identified as a candidate chromosome 11q tumor suppressor gene [20-22].

Chromosome 1p loss Deletion of chromosome 1p sequences is more common in high-stage tumors and is usually associated with MYCN amplification. The prognostic significance of 1p loss has long been controversial but current evidence suggests that allelic loss of 1p36 sequences predicts an increased risk of relapse in patients with localized tumors [18].

Chromosome 17q gain Gain of chromosome 17q is the most common genetic aberration, occurring in approximately 80% of NBs [23]. It often results from unbalanced translocations with chromosome 1p or chromosome 11q [23,24], although other partner chromosomes can be involved. The involvement of chromosome 1 and chromosome 17 in the etiology of NB was further reinforced by the identification of a constitutional balanced t(1;17) translocation in a patient with NB [25].

1.3 MiRNA and their role in tumorigenesis

MiRNAs are non-coding, single-stranded RNAs of ~22 nucleotides and constitute a novel class of gene regulators that are found in both plants and animals. They negatively regulate their targets in one of two ways depending on the degree of complementarity between the miRNA and the target. First, miRNAs that bind with perfect or nearly perfect complementarity to protein coding mRNA sequences induce the RNA-mediated interference (RNAi) pathway. Briefly, mRNA transcripts are cleaved by ribonucleases in the miRNA-associated, multiprotein RNAinduced-silencing complex (miRISC), which results in the degradation of target mRNAs. This mechanism of miRNA-mediated gene silencing is commonly found in plants, but has also been shown to occur in mammals. However, most animal miRNAs are thought to use a second mechanism of gene regulation that does not involve the cleavage of their mRNA targets. These miRNAs exert their regulatory effects by binding to imperfect complementary sites within the 3′ untranslated regions (UTRs) of their mRNA targets, and they repress target-gene expression post-transcriptionally, apparently at the level of translation, through a RISC complex that is similar to, or possibly identical with, the one that is used for the RNAi pathway (Figure 1).

Together with translational control, miRNAs use this mechanism in order to reduce the protein levels of their target genes, but the mRNA levels of these genes are barely affected. The biogenesis of miRNAs has only recently been elucidated. MiRNAs, which generally seem to be transcribed by RNA polymerase II, are initially made as large RNA precursors that are called pri-miRNAs. The pri-miRNAs are processed in the nucleus by the RNase III enzyme, Drosha, and the double-stranded- RNA-binding protein, Pasha (also known as DGCR8), into ~70-nucleotide pre-miRNAs, which fold into imperfect stem-loop structures.
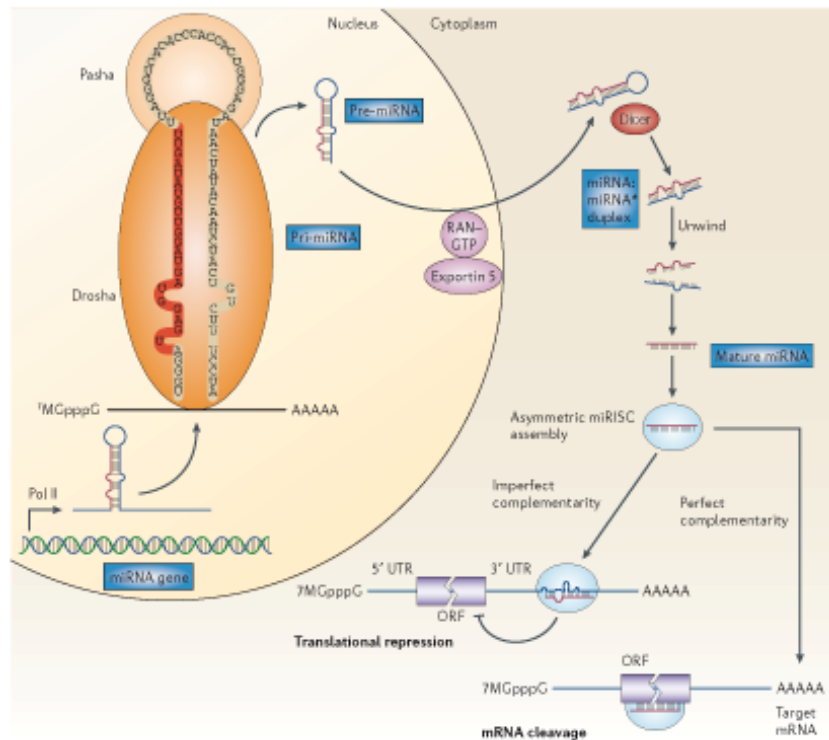
Figure 1: The biogenesis of microRNAs. MicroRNA (miRNA) genes are generally transcribed by RNA Polymerase II (Pol II) in the nucleus to form large pri-miRNA transcripts, which are capped (7MGpppG) and polyadenylated (AAAAA). These pri-miRNA transcripts are processed by the RNase III enzyme Drosha and its co-factor, Pasha, to release the ~70-nucleotide pre-miRNA precursor product. (Note that the human let-7a-1 miRNA is shown here as an example of a pre-miRNA hairpin sequence. The mature miRNA sequence is shown in red.) RAN–GTP and exportin 5 transport the pre-miRNA into the cytoplasm. Subsequently, another RNase III enzyme, Dicer, processes the pre-miRNA to generate a transient ~22- nucleotide miRNA:miRNA* duplex. This duplex is then loaded into the miRNA-associated multiprotein RNA-induced silencing complex (miRISC) (light blue), which includes the Argonaute proteins, and the mature single-stranded miRNA (red) is preferentially retained in this complex. The mature miRNA then binds to complementary sites in the mRNA target to negatively regulate gene expression in one of two ways that depend on the degree of complementarity between the miRNA and its target. miRNAs that bind to mRNA targets with imperfect complementarity block target gene expression at the level of protein translation (lower left). However, recent evidence indicates that miRNAs might also affect mRNA stability (not shown). Complementary sites for miRNAs using this mechanism are generally found in the 3′ untranslated regions (3′ UTRs) of the target mRNA genes. miRNAs that bind to their mRNA targets with perfect (or nearly perfect) complementarity induce target-mRNA cleavage (lower right). miRNAs using this mechanism bind to miRNA complementary sites that are generally found in the coding sequence or open reading frame (ORF) of the mRNA target.

The pre-miRNAs are then exported into the cytoplasm by the RAN GTP-dependent transporter exportin 5 and undergo an additional processing step in which a double- stranded RNA of ~22 nucleotides in length, referred to as the miRNA:miRNA* duplex, is excised from the pre-miRNA hairpin by another RNAse III enzyme, Dicer. Subsequently, the miRNA:miRNA* duplex is incorporated into the RISC complex. The mature miRNA strand is

preferentially retained in the functional RISC complex and negatively regulates its target genes. Many researchers failed to appreciate the importance of miRNAs when they were initially described more than a decade ago. This is because the first miRNA gene that was identified, *lin-4*, was thought to be unique to the roundworm *Caenorhabditis elegans* and control the timing and progression of the nematode life cycle. However, the identification of hundreds of miRNAs within worm, fly and mammalian genomes by traditional cloning techniques and bioinformatics has captured the attention of scientists specializing in various different fields. Most human miRNAs are found within introns of either protein-coding or noncoding mRNA transcripts. The remaining miRNAs are either located far from other transcripts in the genome, within the exons of noncoding mRNA genes or within the 3′ UTRs of mRNA genes, or they are clustered with other miRNA genes, including a cluster on chromosome that is comprised of novel miRNAs. miRNAs can be grouped into families on the basis of sequence homology, which is found primarily at the 5′ end of the mature miRNAs, but whether members of the same miRNA family control similar biological events remains to be seen. Many miRNAs are evolutionarily conserved from worms to humans, which implies that these miRNAs direct essential processes both during development and in the adult body. Several studies have shown a strong correlation between abrogated expression of miRNAs and oncogenesis. Our study recently provided evidences that support this mechanism in the Medulloblastoma (MB) tumors. Indeed, we have recently shown that miR199b-5p, through direct targeting of Hes1 gene, key effector of the Notch pathway, exerts onco-suppressor functions in MB cells. We reported that over-expression of miR199b-5p impairs proliferation of different MB cells and affects survival of the MB stem-cell subpopulation [26]. Another report demonstrated that miR-21 is upregulated in glioblastoma. This gene was found to be expressed at a 5–100-fold higher rate in gliomas than in normal tissue. Antisense studies of miR-21 in glioblastoma cell lines showed that this miRNA controls cell growth by

inhibiting apoptosis but does not affect cell proliferation, which implies an oncogenic role for this miRNA. Finally miR34a expression was reported significantly downregulated in several human cancers, and aberrant CpG methylation of its promoter was observed in prostate carcinomas and primary melanomas, as well as in several tumor cell lines, [27] and loss of miR-34 has been linked to chemoresistance of cancer.
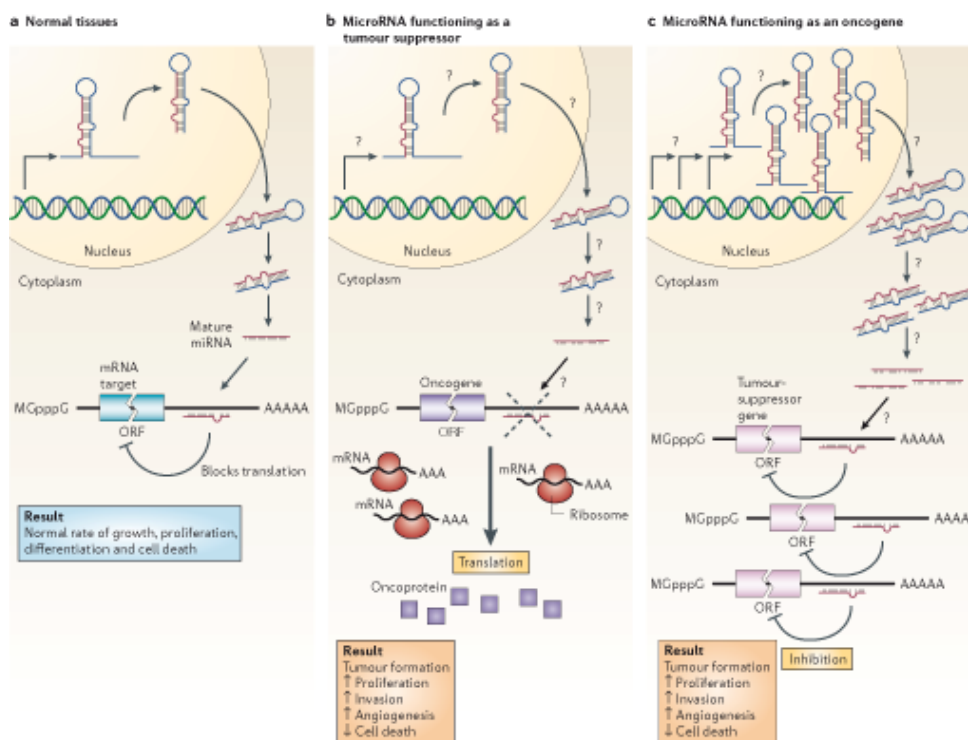

Figure 2: MicroRNAs can function as tumour suppressors and oncogenes. a |In normal tissues, proper microRNA (miRNA) transcription, processing and binding to complementary sequences on the target mRNA results in the repression of target-gene expression through a block in protein translation or altered mRNA stability (not shown). The overall result is normal rates of cellular growth, proliferation, differentiation and cell death. **b** The reduction or deletion of a miRNA that functions as a tumour suppressor leads to tumour formation. A reduction in or elimination of mature miRNA levels can occur because of defects at any stage of miRNA biogenesis (indicated by question marks) and ultimately leads to the inappropriate expression of the miRNA-target oncoprotein (purple squares). The overall outcome might involve increased proliferation, invasiveness or angiogenesis, decreased levels of apoptosis, or undifferentiated or de-differentiated tissue, ultimately leading to tumour formation. **c** The amplification or overexpression of a miRNA that has an oncogenic role would also result in tumour formation. In this situation, increased amounts of a miRNA, which might be produced at inappropriate times or in the wrong tissues, would eliminate the expression of a miRNA-target tumour-suppressor gene (pink) and lead to cancer progression. Increased levels of mature miRNA might occur because of amplification of the miRNA gene, a constitutively active promoter, increased efficiency in miRNA processing or increased stability of the miRNA (indicated by question marks).

1.4 miR-34a

MiR-34 is an evolutionary conserved family of miRNAs consisting of three members in vertebrates (miR-34a, miR-34b and miR-34c), and one orthologue sequence in invertebrates species.

In human, miR-34a precursor sequence maps on the short arm of chromosome 1 in position p36.23; while, miR-34b and miR-34c on long arm of the chromosome 11 in position q23.1 (Figure 3).
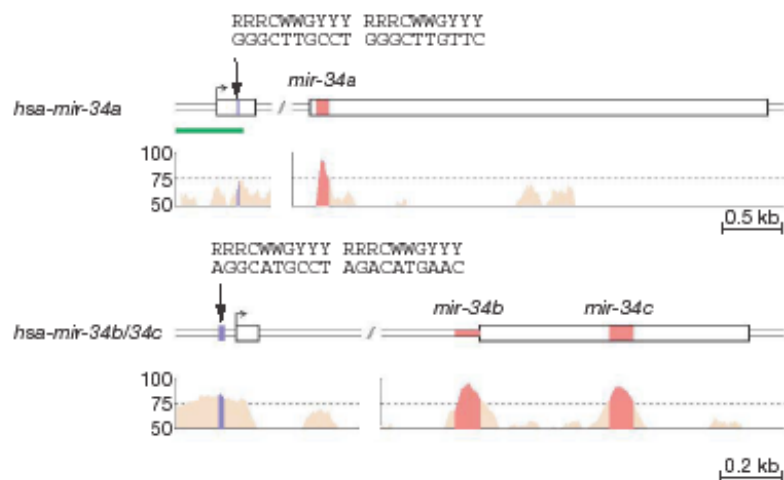

Figure 3: p53 Binding site within promoter region of miR34 Family. Schematic representation of p53 binding sites identified upstream 30Kb and 3kb respectively of the miR34a and cluster miR34b/c loci.

Several groups have recently reported that the three-miR34 family members are direct targets of p53 transcription factor [28]; in particular, miRNA expression profiles of five different studies reported miR-34a as the most significantly induced miRNA after activation of p53.

p53 binding sites were identified 30Kb and 3kb upstream respectively of the miR-34a and cluster miR34b/c loci, and CHIP (chromatin immunoprecipitation) performed had confirmed the p53 binding.

However ectopic expression of miR-34a recapitulated p53 mediated effects including cell cycle arrest and induction of apoptosis and senescence-like phenotype. On the other hand, inhibition of miR-34a functions via specific LNA (locked nucleotide analogs) impaired p53-induced apoptosis, upon DNA

damage induction [29]. Therefore, miR-34a can be, in some cases, not only sufficient but also required for mediation of tumor suppression by p53.

Until now, several miR-34a targets have been experimentally validated, including CDK4/6, cyclin E2, cyclin D1, E2F5, MET, Bcl2, MYCN and SIRT1. The high similarity among the three processed miR34 family members suggested that they might have the same targets. However, miR-34a and the cluster miR34b/c have distinct tissue-specific expression patterns, with miR-34a presents at highest levels in the mouse brain, and low or moderate levels in other tissues, whereas miR-34b and miR-34c most highly expressed in lung [30].

Recently, Ji and colleagues had shown in human pancreatic cancer cell another potential role for miR-34 in cancer initiation and progression linking miR-34a to tumor-initiating cells or cancer stem cells (CSC). Another report demonstrated that, in CD44 marker-positive versus marker-negative prostate cancer cell populations, miR-34a (1p36.22) was prominently under-expressed in all populations while the other two miR-34 family members, miR-34b and miR-34c (11q23.1), did not show consistent differences between these cells. Finally, Guessous has shown that miR-34a reduces glioma stemness and induces cell differentiation into astrocytes, neurons and oligodendrocytes. Remarkably, in situ hybridization analysis of rat organs showed the highest expression of miR-34a within the cerebellum cortex, thus suggesting potential biologic roles of the endogenous miRNA in this brain tissues [31]. Emerging evidence suggests a role for aberrant miRNA regulation in Neuroblastoma. Expression profiling of miRNAs in Neuroblastoma identified miRNA expression signatures that are predictive of clinical outcome. The genes encoding miR34-a at 1p36 and miR-125b at 11q24 are frequently deleted and have been shown to function as tumor suppressors in Neuroblastoma.

1.5 MicroRNAs in the pathogenesis of Neuroblastoma

With the emergence of an additional complex layer of gene regulation through the discovery of microRNAs, there is realistic hope for new insights into the complex pathogenesis of Neuroblastoma, which may finally contribute to solving open questions and enlightening seemingly paradoxical results. Since Neuroblastoma is an embryonal tumor and microRNAs are major regulators of differentiation and development, microRNA analysis bears the potential to deliver new insights into the pathogenesis of this malignancy .

MiRNAs regulate gene expression at a post-transcriptional level by inhibiting mRNAs from being translated or causing them to be degraded. They play major roles in the differentiation of neural cells, and the deregulation of these sequences can contribute to tumorigenesis in many forms of cancer. Expression profiling of miRNAs in Neuroblastomas has identified a number of miRNAs that are differentially expressed in favorable versus unfavorable tumor subtypes, particularly with respect to MNA versus non-MNA tumors. Functional studies have demonstrated that several miRNAs are able to induce apoptosis or differentiation when ectopically over-expressed in Neuroblastoma cell lines. Chen and Stallings [32] demonstrated that many miRNA loci are differentially expressed in different genomic subtypes of Neuroblastoma and that these subtypes can be identified on the basis of miRNA expression patterns. It was further noted that a large number of miRNAs appeared to be down-regulated in the MNA subtype relative to the 11q- or hyperdiploid subtypes, indicating that MYCN might mediate a tumorigenic effect, in part, by down-regulating miRNAs that have pro-apoptotic or pro-differentiation effects. MiR-184 is an example of a miRNA that is down-regulated in the MNA subtype which has pro-apoptotic effects when ectopically up-regulated in Neuroblastoma cell lines. Interestingly, a related transcription factor, MYC, apparently directly down-regulates a number of miRNA loci in other forms of cancer [33]. Fontana et al. demonstrated that the five miRNAs mapping within the miR-17-5p-92 polycistronic cluster (miR-17-5p, -18a, -19a, -20a and -92)

were expressed at higher levels in Neuroblastoma cell lines exhibiting over-expression of MYCN relative to cell lines with low levels of this transcription factor [34]. In particular, tumors of the MYCN amplified (MNA) subtype could be quite accurately classified on the basis of miRNA expression profiling, as illustrated in figure 4.
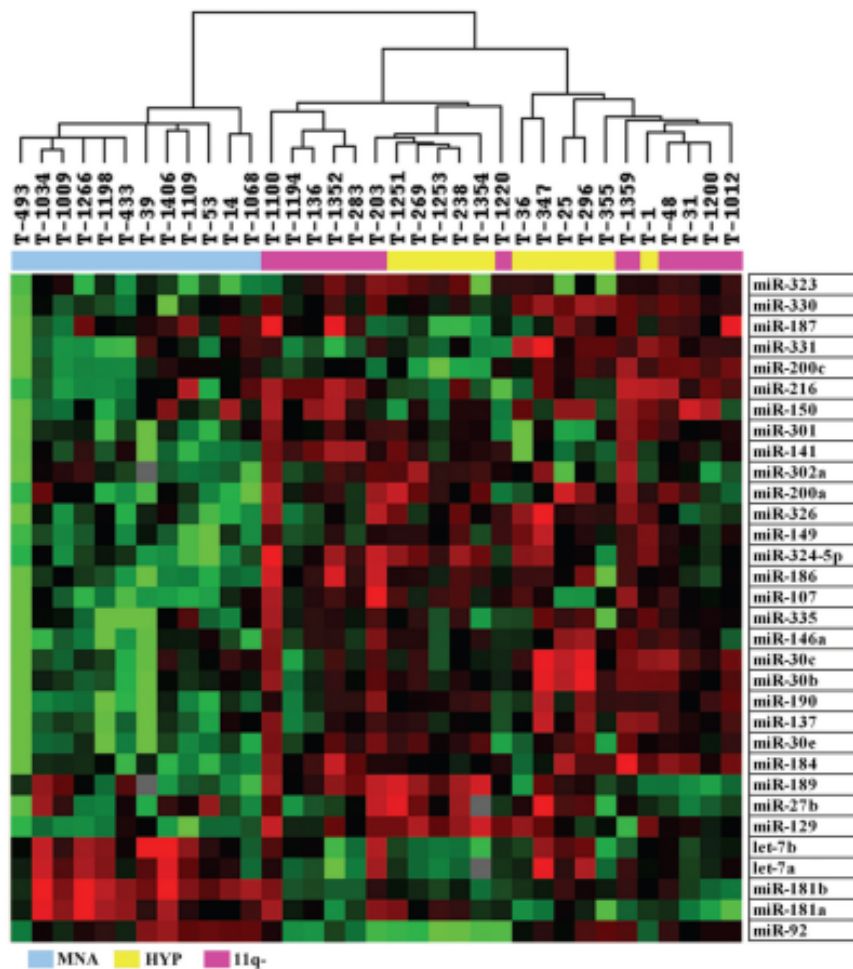

Figure 4. Heat map summarizing the patterns of expression for 32 miRNA loci that were differentially expressed in neuroblastoma tumor subtypes (low stage hyperdiploid tumors with favorable histopathology, yellow; high stage 11q-tumors with unfavorable histopathology, pink; and high stage MYCN amplified tumors with unfavorable histopathology, blue). High expression is indicated by red, while low expression is indicated by green. MYCN amplified tumors form a distinct cluster characterized by low expression levels of many miRNA loci. The 11q- tumors formed two separate clusters, which could not always be perfectly distinguished from the low stage hyperdiploid tumors. This figure and its legend was originally published by Chen and Stallings [32].

In addition to miRNAs behaving in a dominant, oncogenic manner in Neuroblastoma, there is also evidence that miRNAs can act in a recessive, tumor suppressive fashion. The first miRNA identified in Neuroblastoma with tumor suppressor properties was miR-34a. In fact, different studies have demonstrated that miR-34a, mapping to a region on chromosome 1p that is often deleted in high stage disease, acts as a tumor suppressor in Neuroblastoma, as ectopic over-expression of this miRNA decreases cell proliferation through the induction of apoptosis. Using array comparative genomic hybridization (CGH) data on a published set of tumors, Welch and colleagues determined that the region encoding miR-34a is located in the minimal region of 1p loss and demonstrated that the expression of miR-34a was generally reduced in NB primary tumors as compared to normal adrenal gland, and tumors with 1p loss have a 30% reduction in miR-34a expression relative to tumors with an intact 1p locus. Similarly, miR-34a expression is reduced in the majority of NB cell lines tested. Neuroblastomas only rarely harbor p53 mutations, unlike most other tumors. However, attenuation of p53 function may well still be an important step in Neuroblastomagenesis, and achieved via the downregulation of miR-34a through the loss of 1p36.

Aims

Due to the advances and achievements of genomics, the study of proteins encoded by the genome was the next logical step in understanding functional aspects of the cell. Powerful nucleic acid approaches are still limited because DNA sequences and mRNA levels are not sufficient to predict the amount, and activity of the proteins in the cell, moreover the relationships between the levels of transcripts and the levels of the proteins encoded by they, does not always show direct correlation. Proteome is very dynamic and can change in response to cellular or environmental factors. In addition, the proteome is orders of magnitude more complex than the genome due to processes such as splicing, post-translational events at the protein level, post-translational modifications, protein degradation, drug perturbations and disease. Furthermore, differences in protein abundance within the cell vary greatly and the identification of low abundant proteins remains a challenge. Aim of this study is the identification of early direct target of miR-34a in Neuroblastoma, observing changes in protein expression induced by miR-34a. Using quantitative bottom-up proteomics in two different NBL cell lines, we addressed to detected proteins differentially regulated by miR-34a, and among these, identify which are the direct targets, that determine the effects on the inhibition of the multiple tumor pathways by directly and indirectly regulation of numerous critical proteins. Our goal is to determine the complex protein network regulated by miR-34a and the effects resulting from this perturbation on the cellular system.

Moreover, another important issue addressed in this thesis is the identification of time point of regulation (early or late) in which occurs the greater control on protein expression by miR-34a and to demonstrate that miR-34a dinamically regulates the expression of proteins involved in several crucial pathways with a relative importance in tumor progression.

Results 2

2. Results

2.1 Conditional miR-34a expression

One debatable question was related to miR-34a target recognition. At this time several miR-34a target genes have been identified, even though a lot remains to define. Moreover, in deep knowledge the next step will be the understanding how the impairment of miR-34a targets will be exerted on biological pathways, defining in this way networks that are directly or indirectly regulated by miR-34a and this will be of importance for future therapeutic applications.

To identify miR-34a induced changes in protein expression in Neuroblastoma, we generated in two different cell lines, SHEP and SH-SY5Y, several miR-34a tetracycline-inducible clones, based on Tet on system (Figure 5).
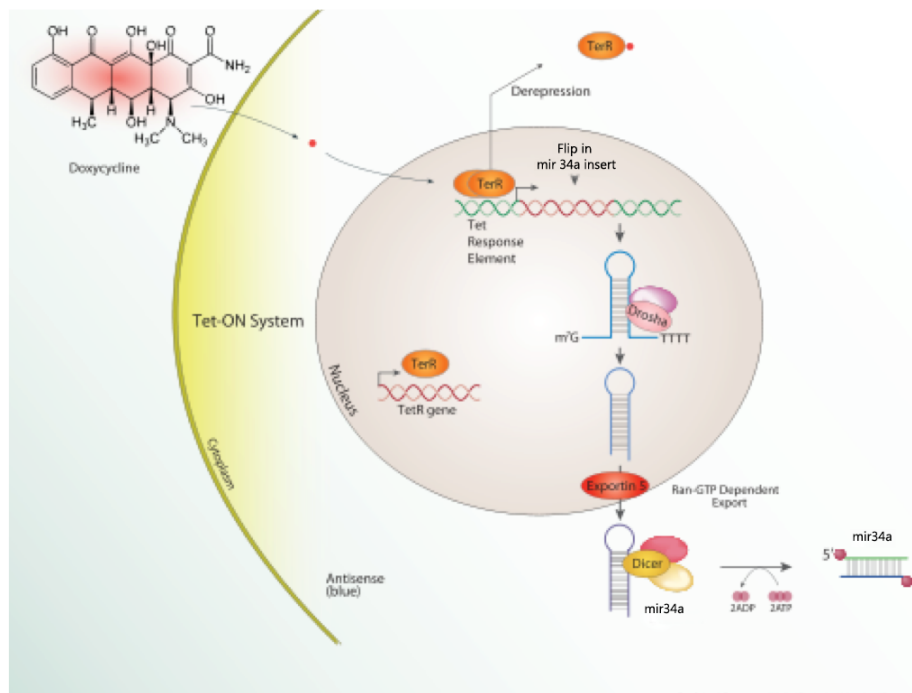

Figure 5. Conditional miR-34a expression. Schematic of the tet-on system in which doxycycline is required for activation of miR-34a expression by rtTA.

This system was important to minimize the variability of microRNA expression during transient transfection and to minimize, during microRNA processing, the side effects on RISC complex obstruction, phenomena that are

often encountered once a given miRNA is constitutively expressed. Ectopic expression of miR-34a in each generated clone was verified by Real Rime PCR methodology. We detected a significant fold increase of miR-34a levels in tetracycline-treated cells at 6 hours after induction compared to the untreated control cells (Figure 6A-B).
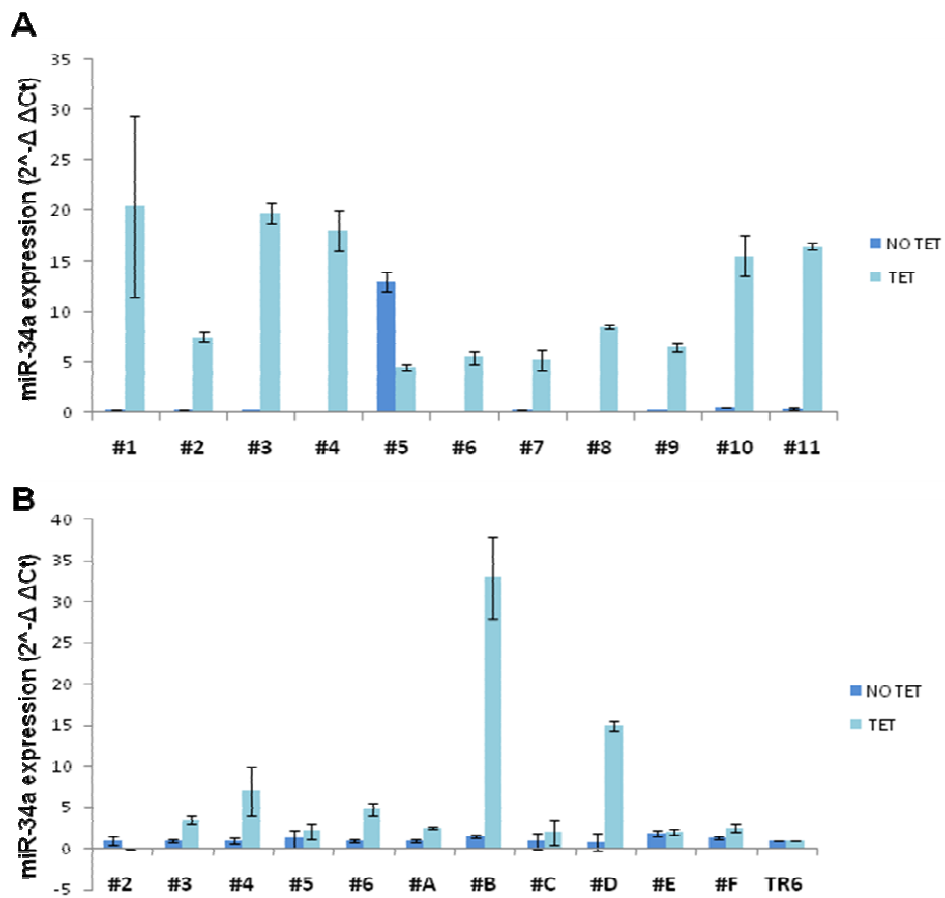

Figure 6. mRNA expression levels of miR-34a in inducible stable clones determined by Q-RT-PCR. The levels of miR-34a expression in SH-SY5Y (A) and SHEP (B) cells were represented as multiples of 2-DCT values compared with non stimulated cells.

Among the analyzed clones, we choose in SHEP cell lines the clone ♯D and for SH-SY5Y cells the clone ♯4. Both these clones showed low levels of endogenous miR-34a and high levels of expression following tetracycline stimulation.

Moreover, to further validate the effect of miR-34a in SH-SY5Y ♯4 cells we checked out the expression levels of the previously identified targets, such as Survivin and Cyclin D3 [35] [36], observing a decreased protein amount after induction of miR-34a expression (see Figure 7). As the ectopic expression of miR-34a resulted in the expected effects in SH-SY5Y cells, we employed these cells for Shotgun analysis with differential labeling.
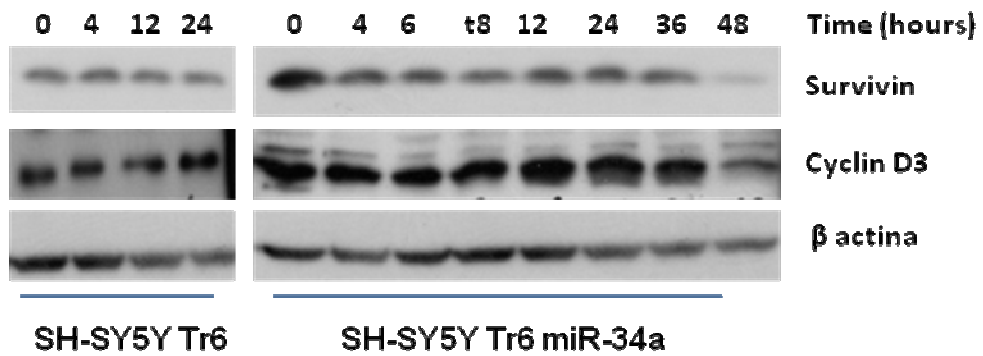

Figure 7. Western blotting showing the protein expression levels of Survivin and Cyclin D3 in SH-SY5Y Tr6 miR-34a compared to empty vector (SH-SY5Y Tr6) at different time points. Anti β-actin was used as the loading control.

2.2 Shotgun analysis with differential labeling

To study the regulatory effects of miR-34a activation, in collaboration with Prof. Kris Gevaert (Vlaams Instituut voor Biotechnologie (VIB), Ghent), quantitative bottom-up proteomics analysis was applied to measure protein response into the previous described cellular models, following induced expression of miR-34a by tetracycline. This approach provides the most wide and relevant readout being it as direct measurement of the miRNA's impact on entire proteome.

To achieve this, SHEP-♯D and SH-SY5Y-♯4-TR-miR-34a clones and their respective controls (Empty vector- inducible clones) were stimulated with tetracycline and cells were harvested at 6, 12 and 24 hours after induction. To compare the empty vector-expressing cells with the miR-34a-expressing cells, post-metabolic labelling with N-hydroxysuccinimide propionate esters was performed:

- Empty vector cells = NHS-propionate ($^{12}C_3$)
- MiR-34a cells = NHS-propionate ($^{13}C_3$)

Once the samples were labelled, a short analyses, based on 10 light and heavy peptide couples, on the Q-TOF Premier mass spectrometer was performed to verify the 1:1 mixing of the labelled samples. Equal amounts of samples were mixed together and fractionated by RP-HPLC (Figure 8). This fractionation is necessary to avoid a too crowded peptide sample for analysis on the LTQ-Orbitrap Velos, a hybrid mass spectrometer incorporating the LTQ Velos™ dual cell linear trap and the Orbitrap™ analyzer. After this fractionation, fractions separated by 20 min were pooled to reduce the number of LC-MS/MS runs. For each comparison (empty vector cells versus miR-34a cells), 20 peptide fractions were analysed on the LTQ-Orbitrap Velos. The results of analyses were obtained as the peptide ratio of the light (L) labelled (Empty vector - $^{12}C_3$) versus the heavy (H) labelled sample (miR-34a- $^{13}C_3$), so:

L/H Ratio > 1   (down-regulated proteins)

L/H Ratio < 1   (up-regulated proteins)

L/H Ratio = 1   (un-regulated proteins).

Prior to calculate ratios, each protein from the acquired data, was identified following stringent criteria. Using Mascot database to filter the significant identification and quantification,, each protein was defined through the identification of at least two unique peptides with confidence settings greater than 99%. These points will be detailed in the following paragraphs.
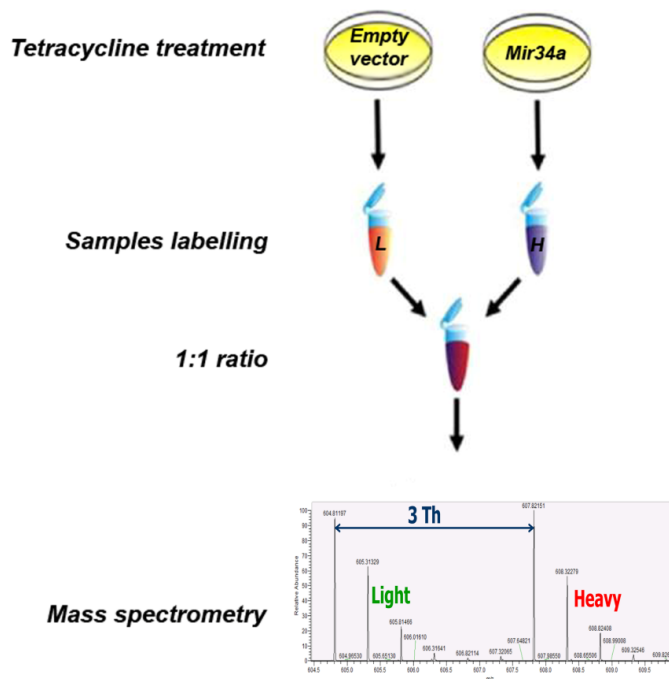

Figure 8. Schematic outline of the post-metabolic labelling with NHS-propionylate (C_{12} and C_{13}) on Lysine (K) and Arginine (R) residues coupled with mass spectrometry analysis. Inducible clones of mir34a (Tet-on system) in two different neuroblastoma cell lines (SHEP and SH-SY5Y) were stimulated with tetracycline to activate miR-34a expression. Once the samples were labelled, samples were mixed together in a 1:1 ratio and were fractionated on a RP-HPLC.

2.2.1 Protein identification using Mascot database

Mascot is a software package from Matrix Science (www.matrixscience.com) that interprets mass spectral data into protein identities. Mascot compares the experimental spectrum against theoretical spectra determined by the in silico

digestion and fragmentation of known proteins in a sequence database. By choosing the best matches between observed and theoretical spectra, Mascot infers the amino acid sequences of the peptides in the sample and then attempts to group together peptide sequences that could come from the same protein. Finally, the protein and peptide identifications are ranked by statistical confidence, and reported. Briefly for each match, between an observed spectrum and an inferred peptide, is assigned a score based on how well the observed spectrum matches the theoretical spectrum for that peptide. This number, named Ions Score, is calculated as -10*Log(P), where P is the probability that the observed match is a random event (Figure 9).

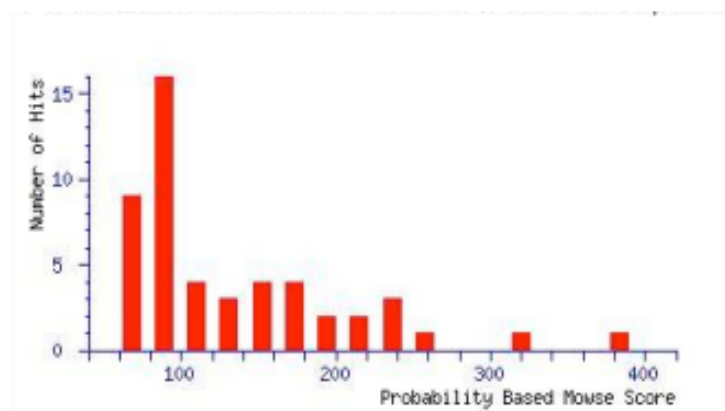**Figure 9.** Ions score is -10*Log(P) where P is the probability that the observed match is a random event. Individuals ions scores > 46 indicate identity or extensive homology (p<0.05). Protein scores are derived from ions scores as a non-probabilistic basis for ranking protein hits.

Some matches will arise simply by chance and Mascot, to address this, calculates a "threshold" score representing a 5% confidence threshold (p value), by calculating for each protein reported, an overall Protein Score. The Protein Score reflects the combined scores of all observed mass spectra assigned to that protein. Protein Scores are non-probabilistic. Further the newer Mascot's release, in its reports include a section called Decoy Search Summary (or False Discovery Rate, depending on which report format is used). The decoy search estimates the number of false peptide identifications by searching

the observed data against a 'decoy' database – a database that is intended to contain only amino acid sequences that are not found in nature. By definition, any match between the data and a sequence in the decoy database is a false-positive. The FDR (false discovery rate) is generally considered a good indication of the quality of the experiment. Since most experiments produce a large number of peptide identifications, a certain percentage of these identifications will, statistically-speaking, be false-positives. For this reason, protein identifications based on multiple matching peptides are generally considered superior to protein identifications based on a single peptide match.

The data obtained from the LTQ-Orbitrap Velos were presented to the Swiss-Prot database, where we searched under the taxonomy "Homo sapiens". To identify the proteins, we linked each sequence to a protein using the Mascot database search engine. The identification was carried out with confidence settings of 99%. This means that the score always had to be higher than or equal to the identity threshold at 99% confidence in order for a peptide identification to be noted valid. Quantification was performed by the Mascot Distiller algorithm. This algorithm provides "true" and "false" quantifications, where the "true" ones are statistically trustworthy, while the "false" ones are not.

2.3 Protein lists and quality control

Despite the raw data have been cleaned up, the reliability of the identification was lifted by adding additional strict filters on the data here analyzed. This means that proteins were considered identified when were supported by at least two peptides, and one of them must be unique, with a minimum length of eight amino acids. By using Knime tool, the data were grouped by sequence and then by accession number. Row data were filtered and finally, six peptide lists and then six protein lists were created, one for each time point of both cell lines (Figure 10).
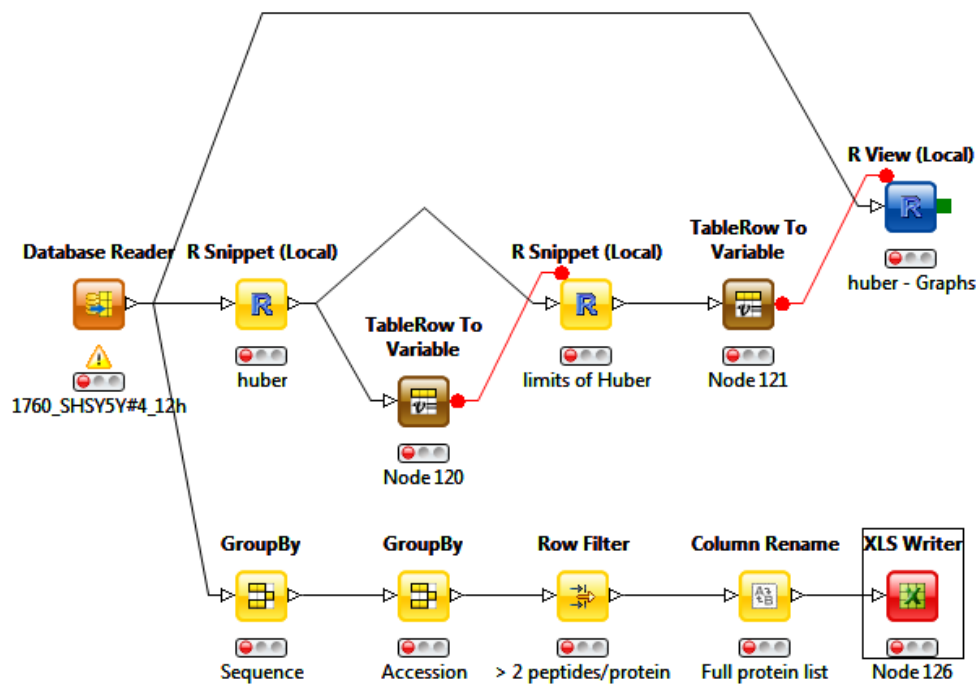
Figure 10. Knime workflow showing the path followed to obtain the protein lists

To check the quality of the analysis, a robust statistical analysis was performed. Tables 1 and 2 show the median and the standard deviation, based on the "true" quantification data in all experiments performed in SHEP and SH-SY5Y cell lines respectively:

	SHEP empty vector vs. SHEP miR34a #D at time point 6h (log2)	SHEP empty vector vs. SHEP miR34a #D at time point 12h (log2)	SHEP empty vector vs. SHEP miR34a #D at time point 24h (log2)
Median	0,105	0,006	-0,315
Standard deviation	0,462	0,297	0,327

Table 1. Median and standard deviation based on the "true" quantification data of the SHEP empty vector versus SHEP miR34a #D at different time points.

	SH-SY5Y empty vector vs. SH-SY5Y miR34a #4 at time point 6h (log2)	SH-SY5Y empty vector vs. SH-SY5Y miR34a #4 at time point 12h (log2)	SH-SY5Y empty vector vs. SH-SY5Y miR34a #4 at time point 24h (log2)
Median	-0,238	-0,08	-0,794
Standard deviation	0,315	0,285	0,279

Table 2. Median and standard deviation based on the "true" quantification data of the SH-SY5Y empty vector versus SH-SY5Y miR34a #4 at different time points.

The median represents how well the mixing of the light and heavy labelled sample was performed, while the standard deviation shows how narrow the distribution is. For example, in SHEP #D experiment (time point 12h) we obtain a median close to 0 (0.006) and a low standard deviation (0.297), which are indications for a good experiment in terms of labelling and mixing. The same statistical data are shown in figure 11.
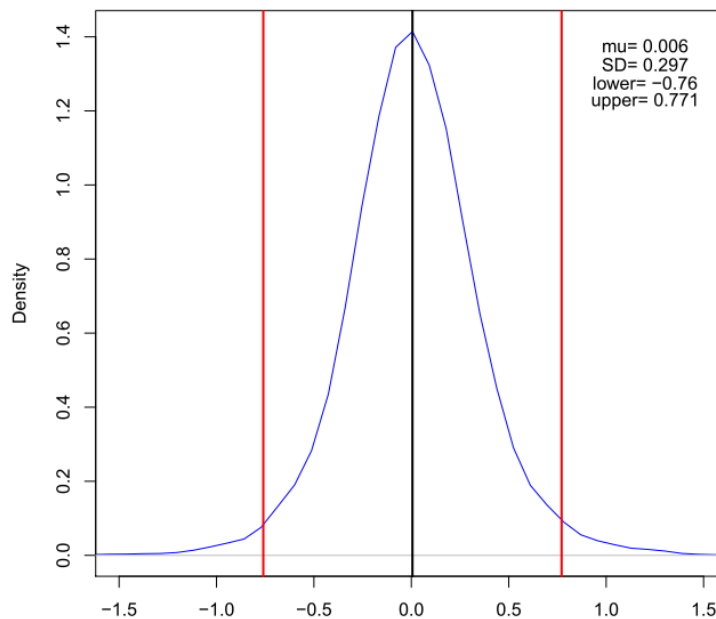

Figure 11. Normal distribution based on the "true" quantification data of the SHEP empty vector vs. SHEP miR-34a #D cells at time point 12h. The black line represents the median and the 2 red lines are the outliners calculated on a 99% confidence interval (µ ± (2.58 * SD) = -0.76 and 0.771).

2.4 Changes in protein expression induced by miR-34a over-expression at 6 hours

In order to identify early targets of miR-34a, we firstly focused our attention on the differentially expressed proteins at 6 hr after tetracycline induction in both NBL cell lines. To achieve this, the protein expression data were filtered based on the ratios: proteins with ratios higher than upper limit were considered down-regulated, while those with ratios less than the lower limit were considered up-regulated. The outlines were calculated on a 99% confidence interval. In detail, the area bounded by red lines represents the middle 99% of the distribution and stretches from -1.043 to 1.348 in SHEP (Fig. 12A) and from -1.05 to 0.575 in SH-SY5Y (Fig. 12B).
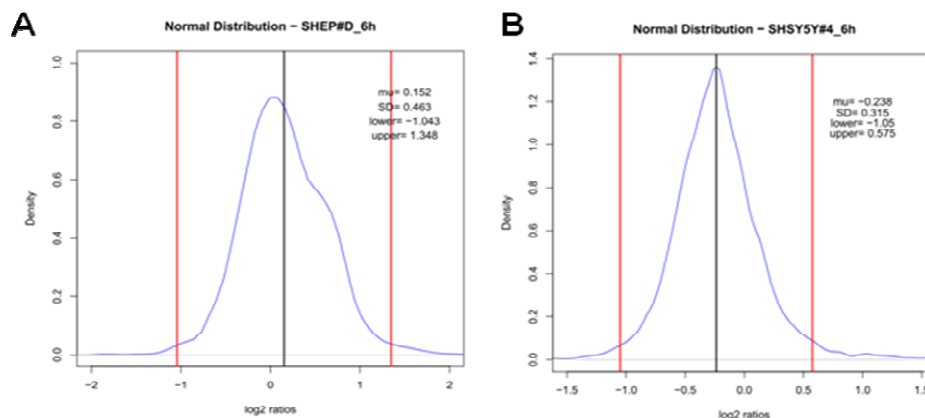

Figure 12: Normal distribution based on the "true" quantification data of the SHEP empty vector vs. SHEP miR34a #D (**A**) and SH-SY5Y empty vector vs. SH-SY5Y miR34a (**B**) cells at time point 6h. The black line represents the median and the 2 red lines are the outliners calculated on a 99% confidence interval ($\mu \pm (2.58 * SD)$).

These limits were computed by adding and subtracting 2.58 standard deviations to/from the mean (μ) as follows:

$$(\mu) - (2.58)(SD) = \text{lower limit}$$
$$(\mu) + (2.58)(SD) = \text{upper limit}$$

The value of 2.58 was used according to 99% of confidence. The area of a normal distribution is within $\pm$ 2.58 standard deviations of the mean; where SD is the standard error of the mean.

Applying these computations, we observed in SHEP (log2 ratio < -1.043) and in SH-SY5Y (log2 ratio < -1.05) cells lines, respectively 4 and 17 proteins up-regulated. Analyzing the protein that are negatively regulated, we found 21 down-regulated proteins in SHEP cells (log2 ratio > 1.348) and 59 in SHSY-5Y cells (log2 ratio > 0.575) (Figure 13A) . The overlap of proteins down-regulated in both of these cell lines was 5 proteins (CO1A1, PLEC, PTRF, VIME and RRMJ3), as shown in Venn diagram below. A graphical summary of protein expression changes resulting by miR-34a expression is presented in figure 13B.
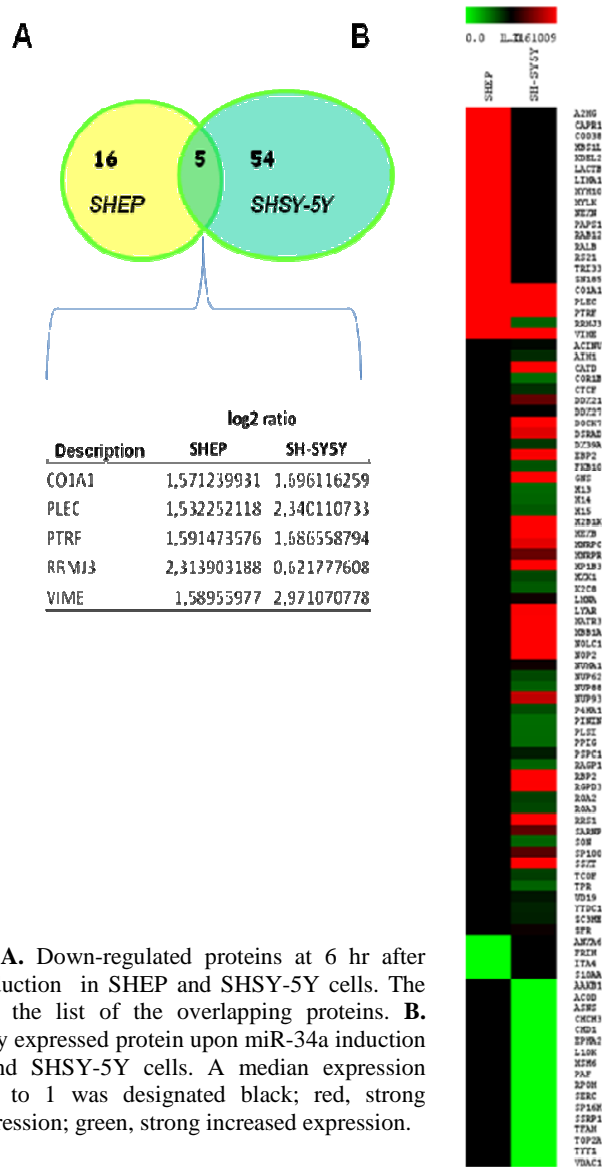

Description	log2 ratio	
---	SHEP	SH-SY5Y
CO1A1	1,571239931	1,696116259
PLEC	1,532252118	2,340110733
PTRF	1,591473576	1,686558794
RRMJ3	2,313903188	0,621777608
VIME	1,58955977	2,971070778

Figure 13. A. Down-regulated proteins at 6 hr after miR-34a induction in SHEP and SHSY-5Y cells. The table shows the list of the overlapping proteins. **B.** Differentially expressed protein upon miR-34a induction in SHEP and SHSY-5Y cells. A median expression value equal to 1 was designated black; red, strong reduced expression; green, strong increased expression.

In order to determine which biological processes (or molecular function) might be predominantly affected in the set of proteins that were significantly changed by miR-34a overexpression (6 hrs) in each NBL cell line, we performed a Gene Ontology analysis. As shown in figure 14, proteins down-regulated by miR-34a in SHEP are involved in cytoskeleton organization (18%), apoptosis (8%), regulation of transcription (5%), signal transduction (20%), cell motility and adhesion (18%), cell division and differentiation (8%).
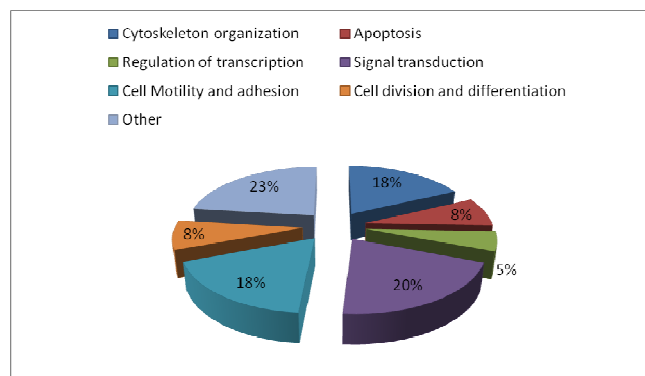

Figure 14. Functional distribution by GO analyses of down-regulated proteins at 6 hr after miR-34a induction in SHEP cell line.

Meanwhile, the functional distribution of down-regulated proteins in SHSY-5Y (Figure 15) are: apoptosis (47%), cell division and differentiation (11%), cell motility and adhesion (14%) and mRNA processing (20%).
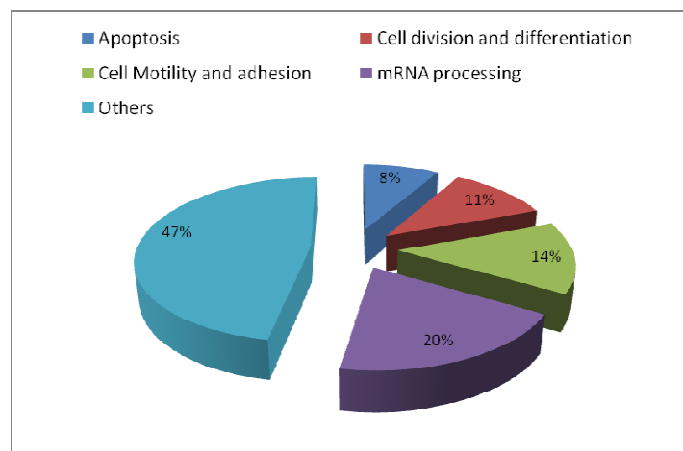

Figure 15. Functional distribution by GO analyses of down-regulated proteins at 6 hr after mir-34a induction in SHSY-5Y .

Many miRNA targets contain a perfect match to the miRNA seed region in their 3' UTR. We speculated that genes encoded for the 5 overlapping proteins have a high probability being direct miR-34a targets. So, to understand if these proteins are direct targets of miR-34a, seeing as the *"condicio sine qua non"* to be a target, is the presence of base pairing into the 3'UTR, we searched in these transcripts the seed sequences for miR-34a. By using PITA (Probability of Interaction by Target Accessibility), a bioinformatics microRNA target prediction tool, we found that miR-34a could potentially targets PLEC (Plectin), PTRF (Polymerase I and transcript release factor), RRMJ3 (Putative rRNA methyltransferase 3) and VIME (Vimentin). For CO1A1 (Collagen alpha-1chain) we did not find seed sequence for miR-34a in the 3'UTR, probably because it might be directly targetable in the 5'UTR or CDS sequences, or most likely because the annotated 3'UTR was incorrect.

Plectin is a large protein (>500 kDa) of the spectrin superfamily that has long been recognized for its ability to bind and link together the three main components of the cytoskeleton: actin, microtubules and intermediate filaments [37]. Plectin is known to bind integrin α6β4 as the major structural proteins of the hemidesmosome, a structure that anchors cells to the extracellular matrix [38]. Recently plectin was identified as a putative biomarker in pancreatic cancer [39,40].

PTRF plays an important role in caveolae formation and organization. Guha and colleagues demonstrated that PTRF might be a potentially important component of the ERBB signaling network [41].

Little is known about RRMJ3 (also called FTSJ3). FTSJ3 is a nucleolar protein involved in Pre-rRNA processing [42].

Vimentin, a major constituent of the intermediate filament family of proteins, is ubiquitously expressed in normal mesenchymal cells and is known to maintain cellular integrity and provide resistance against stress. Vimentin is overexpressed in various epithelial cancers, including prostate cancer, gastrointestinal tumors, tumors of the central nervous system, breast cancer,

malignant melanoma, and lung cancer. Vimentin's overexpression in cancer correlates well with accelerated tumor growth, invasion, and poor prognosis; however, the role of vimentin in cancer progression remains obscure. In recent years, vimentin has been recognized as a marker for epithelial–mesenchymal transition (EMT).

Taken together, these results show that miR-34a directly targets PLEC, PTRF, RRMJ3 and VIME 3'UTR, thus leading to early down-regulation of the encoded proteins in both NBL cell lines. Our data also suggest that miR-34a inhibits either directly or indirectly signal transduction factor and the expression of genes needed for cell proliferation, apoptosis and cell motility.

2.4.1 Analysis of proteins down-regulated by miR-34a at 12 hours

The next step in our investigation was define the effect of miR-34a expression on proteome at later time point. For this purpose, we examined the effect of miR-34a on proteome 12 hours later the induction. As shown in figure 16, we found 26 and 23 significantly down-regulated protein, respectively in SHEP and SHSY-5Y. Among these, only one (CO1A1), was already found down-regulated at 6 hours, in both cell lines.
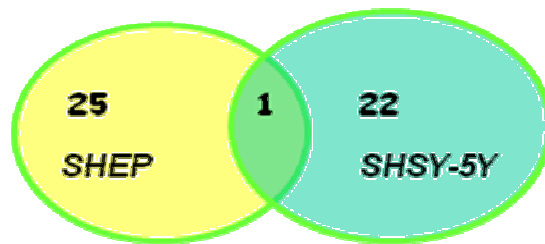

Figure 16. Overlap of down-regulated proteins at 12 hr after mir-34a induction in SHEP and SHSY-5Y cells.

Considering that the directly regulated genes might vary considerably from cell type to cell type or even in the same cell lineage depending on differentiation state or environmental conditions, we next combined all the results generated by Shotgun analysis at 6 and 12 hours in both cell lines. In this way, we obtained a set of 114 proteins regulated by miR-34a:

$$\{\text{Proteins }_{\text{SHEP-6H}}\} \cup \{\text{Proteins }_{\text{SHEP-12H}}\} = \{ \text{Proteins }_{\text{SHEP-6H/12H}}\}$$

$$\{ \text{Proteins }_{\text{SHSY5Y-6H}}\} \cup \{ \text{Proteins }_{\text{SHSY5Y-12H}}\} = \{ \text{Proteins }_{\text{SHSY5Y-6H/12H}}\}$$

$$\{ \text{Proteins }_{\text{SHEP-6H/12H}}\} \cup \{ \text{Proteins }_{\text{SHSY5Y-6H/12H}}\} = \{114 \text{ Proteins}\}$$

Then, sorting this protein set for the presence of miR-34a seed-matching sequences in the 3' UTR of their transcripts, we observed that miR-34a could regulate the 3' UTR of 74.9% of this set of proteins. Considering arbitrarily significant only prediction sites with ΔΔG values less than -10 (energy-based score for microRNA-target interactions equal to the difference between the free

energy gained by the binding of the microRNA to the target, ΔGduplex, and the free energy lost by unpairing the target-site nucleotides, ΔGopen. [43]) , we found 33 genes enriched for miR-34a seed sequence (Table 3).

Accession	Description	Median of the ratio	Median of the ratio (log2)	Sites	ΔΔG Score
P19367	HXK1	1,6534475	0,725477238	6	-21,07
O15231	ZN185	3,045085	1,6064825	5	-16,74
Q9UG63	ABCF2	1,7913675	0,841061337	7	-15,73
P15586	GNS	2,66	1,411426246	5	-15,39
P40261	NNMT	1,9945475	0,996061482	4	-15,31
Q15746	MYLK	3,28683	1,71669684	10	-15,13
P07858	CATB	1,64131	0,714847751	9	-14,68
P30419	NMT1	1,933775	0,951419943	12	-14,57
P46013	KI67	1,785035	0,835952362	8	-14,46
P46060	RAGP1	1,527315	0,61099764	2	-13,55
P13928	ANXA8	2,46724	1,30289806	3	-13,51
Q9H307	PININ	1,49207	0,577315221	2	-13,51
Q9NP73	ALG13	2,547845	1,349277513	1	-13,07
O95340	PAPS2	1,74119	0,80007364	6	-12,85
Q8WX93	PALLD	1,9598175	0,970719316	9	-12,72
P06396	GELS	2,549375	1,350143602	3	-12,71
P13796	PLSL	4,101515	2,036156905	3	-12,71
Q14651	PLSI	1,49661	0,58169832	4	-12,56
P21980	TGM2	2,23097	1,157671114	6	-12,43
Q9Y4K1	AIM1	1,78527	0,836142281	5	-12,31
Q13510	ASAH1	1,690365	0,757334801	2	-12,1
Q96MU7	YTDC1	1,8215025	0,865128975	5	-11,97
P35659	DEK	1,70739	0,771792635	2	-11,95
Q7Z6K5	CO038	59,93468	5,905319126	6	-11,46
Q6P1J9	CDC73	181,0392375	7,500158603	3	-11,46
P07339	CATD	2,08313	1,058752875	3	-11,33
P09486	SPRC	1,77786	0,830141722	5	-11,3
Q9NX58	LYAR	2,3192625	1,213666117	1	-10,66
Q6WKZ4	RFIP1	1,7212	0,783414745	8	-10,39
Q8WU90	ZC3HF	65,84391	6,040978105	2	-10,28
Q9Y5L4	TIM13	7,74423	2,953121801	4	-10

Table 3. List of 33 genes enriched for miR-34a seed sequence.

Then to improve our target prediction functionality in NBL progression, we screen these genes/protein for the correlations of their expression with clinical
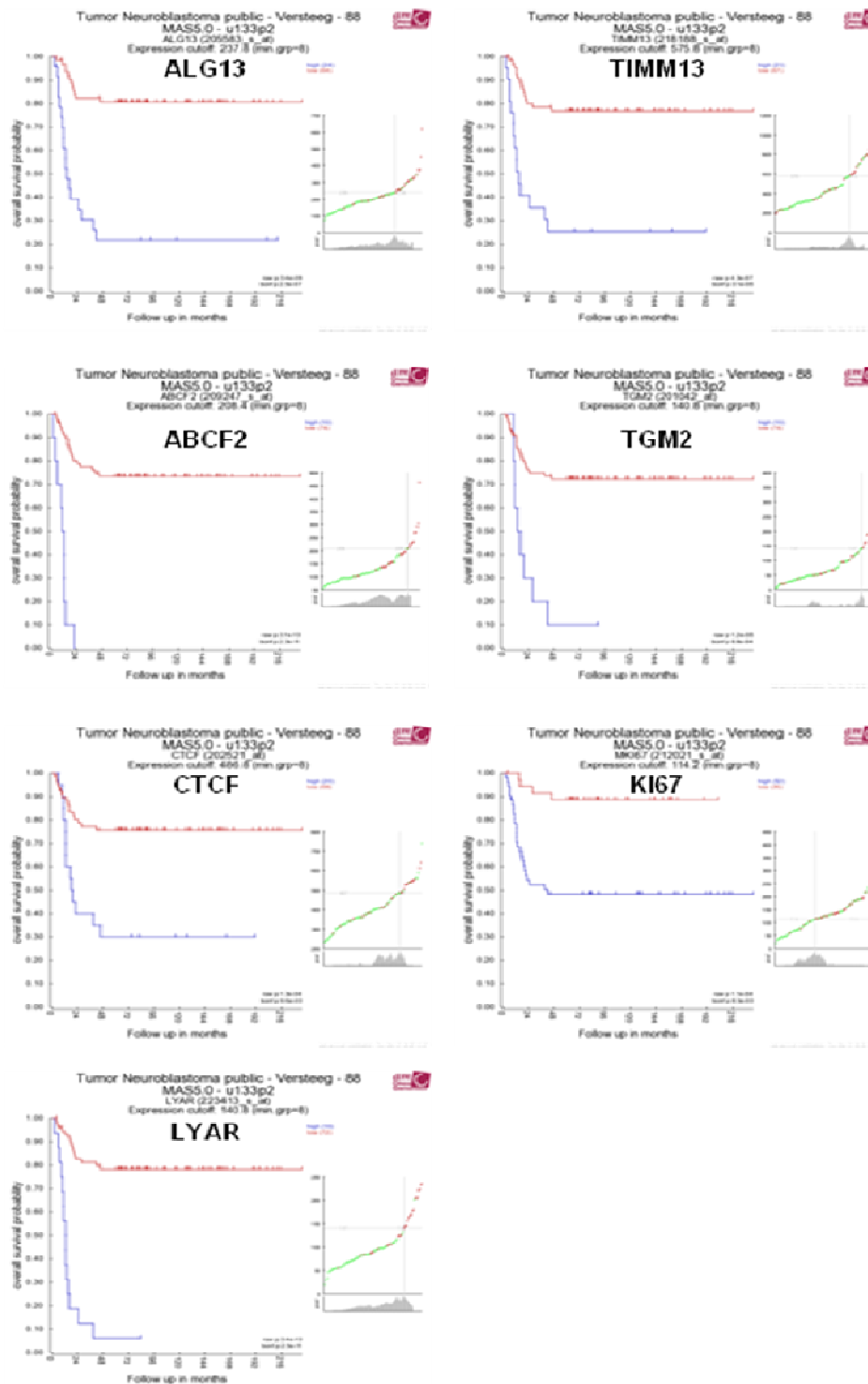

Figure 17. Expression levels of LYAR, CTCF, TGM2, Ki67, TIMM13, ALG13 and ABCF2 correlation to bad clinical outcome in NBL.

outcome of NBL patients searching through a public gene expression database (http://r2.amc.nl). For this reason further efforts have been addressed to verify if any of these genes were correlated to NBL progression and as such would be good candidate to further assign a role of miR34a on their regulation.

Using this flowchart we revealed that, among those analyzed, only n.7 genes correlated to worse clinical outcome when overexpressed in NBL (Figure 17). These genes are involved in the differentiation (LYAR, CTCF), apoptosis and proliferation (TGM2, Ki67), molecular transport (TIMM13 and ABCF2) and several metabolic pathway (ALG13).

To improve the accuracy of target prediction we used other two target prediction algorithms: TargetScan and miRanda. We selected as putative transcripts regulated by miR-34a, 3'UTR with binding sites for miR-34a predicted by at least two of the three bioinformatics algorithms used. Interestingly, the seven targets identified that correlated with poor prognosis in NBL, were predicted as putative target of miR-34a by at least two of the three algorithms used. To test whether the 3' UTR of each gene could be regulated by miR-34a, the 3' UTR of each gene was cloned downstream a luciferase reporter plasmid, and a dual luciferase reporter assay was performed. The data obtained confirmed that miR-34a repress the expression of these genes.

LYAR a nucleolar protein, named Ly-1 antibody reactive clone, encodes a polypeptide consisting of 388 amino acid residues with a zinc finger motif and three copies of nuclear localization signals. The cDNA of LYAR was initially isolated from a mouse T-cell leukemia line more than a decade ago. LYAR cDNA overexpression in NIH-3T3 fibroblast cells rendered them more tumorigenic, indicating that LYAR is a novel nucleolar protein that can be involved in cell growth regulation [44]. Recently, microarray data showed that LYAR is highly expressed in undifferentiated human ESCs and is significantly downregulated upon differentiation [45]. Thus, LYAR appears to be a likely candidate for the study of the involvement of nucleolar mechanisms in

controlling the selfrenewal of ESCs. Hui Li and colleagues demonstrated that Lyar downregulation significantly reduces the rate of ESC growth and increases their apoptosis. Moreover, reduced expression of LYAR in ESCs impairs their differentiation capacity, failing to rapidly silence pluripotency markers and to activate differentiation genes upon differentiation [46].

Our data indicated that Lyar was down-regulated in SHSY-5Y cells at 6 hr after tetracycline induction of miR-34a and, searching in the 3' UTR sequences of Lyar gene, we found potential binding sites of miR-34a.

CTCF is a highly conserved zinc finger protein implicated in multiple regulatory functions, including transcriptional activation/repression, insulation, imprinting, and X chromosome inactivation. Various studies reported that CTCF is involved in cell cycle arrest, apoptosis, and differentiation processes, with the consequence to consider CTCF a potential tumor-suppressor factor. But, other studies reported that CTCF protein levels are elevated in both breast and lung tumoral cell lines [47,48] and, at least in breast cancer cells, CTCF is also associated with apoptosis resistance [47]. These controversial results can be elucidated by the role of CTCF as "differentiation-inducing" factor, involving disparate pathways depending by cellular context [49-51].
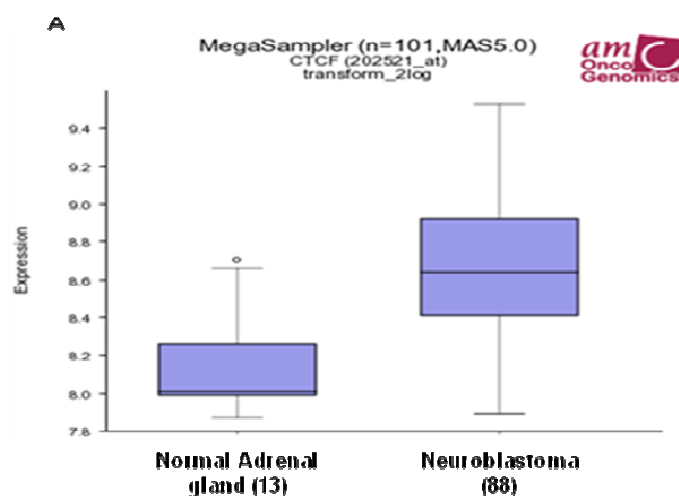

Figure 18. To determine the expression levels of CTCF in human NBL, we searched through a public database (http://r2.amc.nl). This search revealed that is significantly overexpressed in NBL tissues compared to normal adrenal gland (p = 2.2 e^{-6})

In fact, it is assumed that each tumoral cell partially possesses the epigenomic and proteomic features of its physiological counterpart together with crucial alterations that mold its molecular homeostasis and determine CTCF's outcome.

To determine the expression levels of CTCF in human NBL, we searched through a public database of gene expression (http://r2.amc.nl), and we found that CTCF is significantly overexpressed in NBL tissues compared to normal adrenal gland (p = 2.2 e^{-6}) (Fig.18A).

TGM2 (TG2) Tissue transglutaminase is an important member of the transglutaminase family of enzymes that catalyze Ca 2+ -dependent post-translational modification of proteins. Involvement of TG2 in apoptosis has been well established; overexpression of TG2 results in either spontaneous apoptosis of cells or rendering cells highly sensitive to apoptosis-inducing agents. In contrast with this, recent evidence indicates that increased expression of TG2 may prolong cell survival by preventing apoptosis [52].

TG2 expression is upregulated in drug-resistant and metastatic cancer cells and plays a role in the constitutive activation of NF- kB. Increased expression of TG2 contributes to increased survival, invasion and motility of breast cancer cells [53], cell growth and survival in colorectal cancer [54]. A recent study demonstrated that TGF-β-induced TG2 enhances ovarian tumor metastasis by inducing EMT and a cancer stem cell phenotype [55].

Our data demonstrated that miR-34a leads to a direct down-regulation of TGM2 in SHEP cell at 12 hr after induction. Gene expression data revealed that TGM2 is overexpressed in advantage stages of NBL (p=2.1e-03), as shown in figure 19.
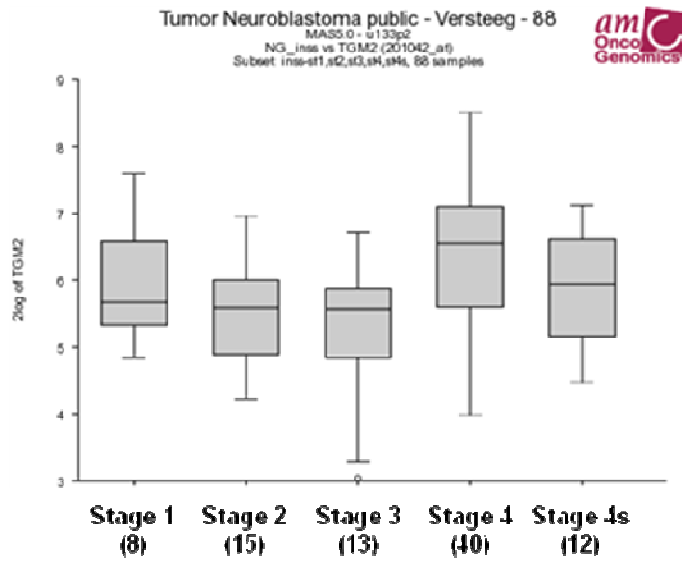
Figure 19. Expression levels of TGM2 in different stages of human NBL.

ABCF2 The ATP binding cassette (ABC) transporter family acts as an efflux pump and its members are related to chemoresistance. ABCF2 is a member, which has a chromosome gain at 7q 34-36. Overexpression of ABCF2 was found in a chemoresistance clear cell ovarian carcinoma and it was also suggested that ABCF2 may contribute to the chemoresistant phenotype [56]. Moreover, ABCF2 protein may be a prognostic marker for ovarian clear cell ovarian adenocarcinoma since that higher ABCF2 DNA and mRNA copy number and protein levels were found in clear cell cases compared with those in serous cases [57]. As shown in figure 20, gene expression data revealed that also ABCF2 was found overexpressed in advantage stages of NBL (p=1.9e-03).
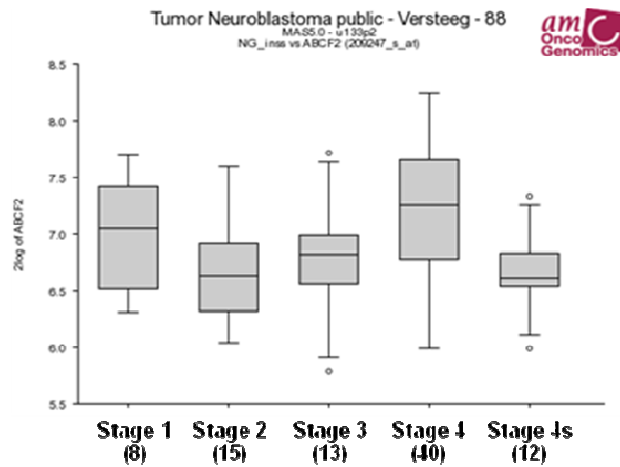
Figure 20. Expression levels of ABCF2 in different stages of human NBL.

KI67 Ki-67 is a protein that in humans is encoded by the MKI67 gene. Antigen Ki-67 is a nucleus protein that is strictly associated with and may be necessary for cellular proliferation. It was recently reported that Ki67 might be suitable for including in the routine clinical practice of breast cancer. For example, Ki67 independently improved the prediction of treatment response and prognosis in a group of breast cancer patients receiving neoadjuvant treatment. A recent study demonstrated that the distribution pattern of Ki67 may be a new independent prognostic factor for breast cancer [58].
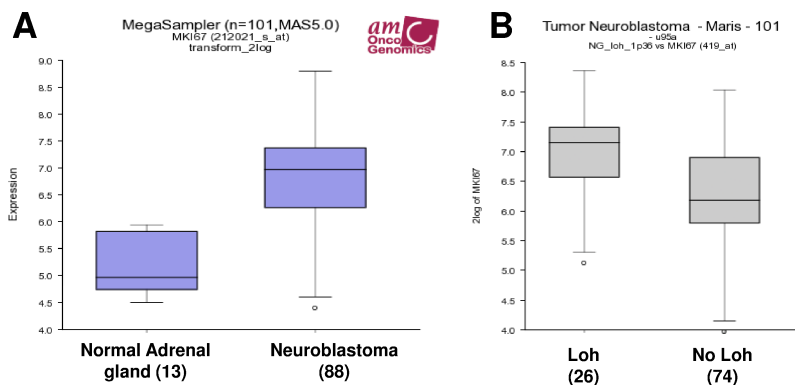

Figure 21. A. Ki67 expression in Neuroblastoma tissues compared to normal adrenal gland (p=9.0 e-11). **B.** Ki67 expression in patients with and without 1p36 loss.

Ki67 was found overexpressed in Neuroblasoma tissues compared to normal adrenal gland (p=9.0 e-11), as shown in figure 21A. Interestingly, in a cohort of Neuroblastoma, we observed that patients showing 1p36 loss have high expression of Ki67 compared to patients without 1p36 (Fig. 21B)(p=2.4e-03). These findings support the notion that Ki67 is regulated by miR-34a.

TIMM13 a member of the "small Tim protein" family, that together with Tim8, forms a soluble hexameric 70 kDa complex in the IMS [59]. This complex is involved in the import of a number of inner membrane proteins. Timm13 is a translocase with similarity to yeast mitochondrial proteins that are involved in the import of metabolite transporters from the cytoplasm and into the mitochondrial inner membrane.

ALG13 is a subunit of a bipartite UDP-N-acetylglucosamine transferase. It heterodimerizes with asparagine-linked glycosylation 14 homolog to form a functional UDP-GlcNAc glycosyltransferase that catalyzes the second sugar addition of the highly conserved oligosaccharide precursor in endoplasmic reticulum N-linked glycosylation. Alg13, as well as Ki67, is highly expressed in patients with 1p36 loss (p= 1.1e-03), tumors wherein that there was a loss miR-34a genetic locus (Figure 22).

Tumor Neuroblastoma - Maris - 101
- u95a
NG_loh_1p36 vs ALG13 (38490_r_at)
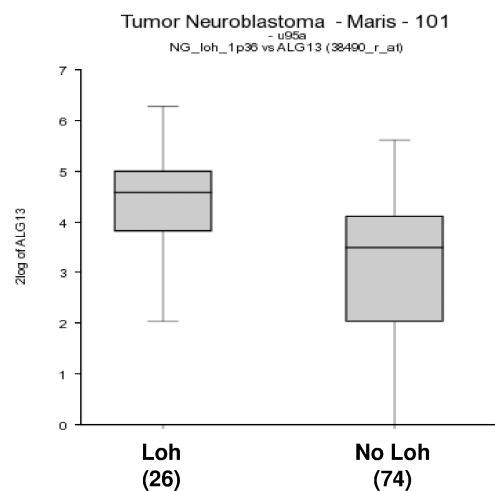
Figure 22. Alg13 expression in patients with and without 1p36 loss.

Overall, the importance of the identification of those seven proteins/genes found down regulated in NBL upon miR-34a expression is of importance because they can be those alternative proteins which may have a role in NBL. Further biological functionality mechanistic mode of actions are needed at this stage to address those independent protein action within a therapeutic intervention of miR34a in the near future.

2.4.2 miR-34a regulates a dense network of genes involved in signal transduction

Additionally, biocomputing analyses are then performed to define whether the genes regulated by miR-34a together acts in a complex network of molecular pathways. To this end, we generated an interactome using the above identified proteins. Using MIMI plug-in of Cytoscape program, that retrieves molecular interactions [55], we found, as shown in figure 23, that LYAR, TGM2, CTCF, TIMM13 and ki67 are strongly linked each other and in turn are linked to the components of molecular signaling cascade, already known to be involved in Neuroblastoma progression, such as Src-Fyn, Lyn, Myc-p53, Tgf-β, IGF and Wnt.
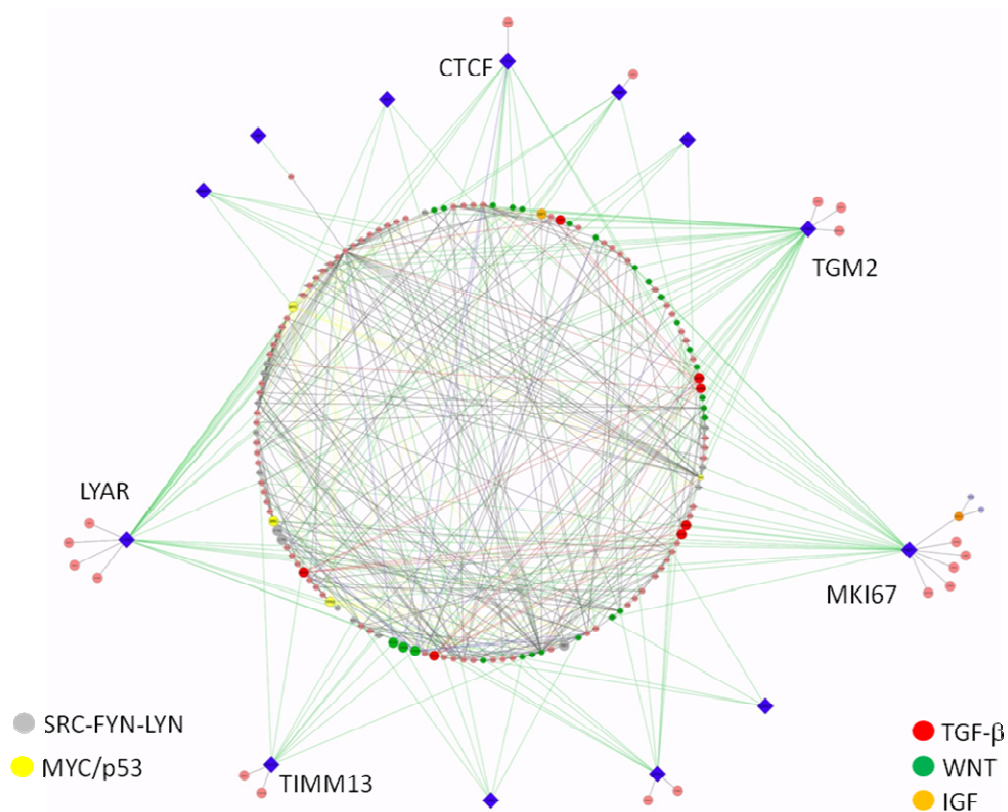

Figure 23. Interactome of LYAR, TGM2, CTCT, TIMM13 and ki67, obtained using MIMI plug-in of Cytoscape program.

Many of these pathways converge on common downstream effectors that were well-established linked to cancer. To verify the effective down-regulation of

these pathways, we evaluated by Western blotting analysis the WNT pathway activation levels in both NBL cells following miR-34a induced expression. For this purpose we treated SH-SY5Y and SHEP cells with tetracycline and harvested the cells at different time points (6-12-24-48 hrs). We then analyzed the expression of activated β-Catenin by using an antibody which is known to recognize amino acid residues (aa36-aa44) of human β-Catenin, specific for the active form. As shown in Figure 24A, the expression of active β-catenin was reduced at 6 hours in SH-SY5Y Tr6 miR-34a#4 compared to SH-SY5Y Tr6 at the same time. Similarly, the amount of activated β-Catenin in SHEP Tr6 miR-34a#D was reduced at 6 and 12 hours and, in the following hours, we did not observed substantial variation on activation compared to control cells.
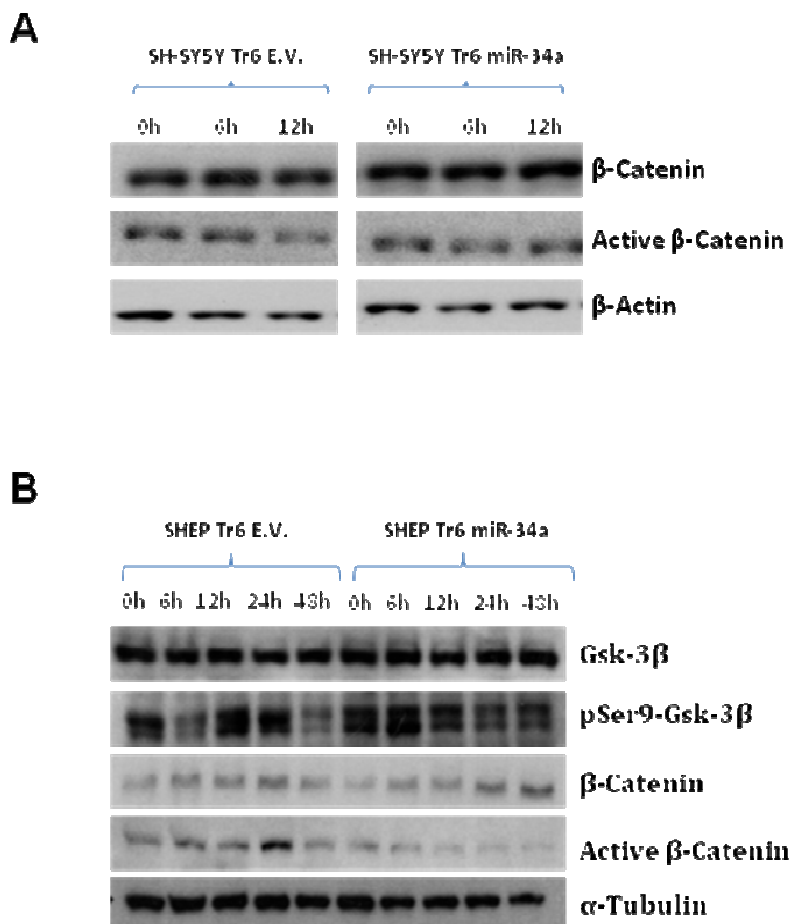

Figure 24. Total protein extracts prepared from SH-SY5Y Tr6 (A) and SHEP (B) Empty vector (E.V.) or -miR-34a overexpressing treated with tetracycline for different time points (6hr, 12hr, 24hr) were subject to Western blotting to evaluate Wnt pathway activation. β-Actin (A) and α-Tubulin were used as loading controls.

Literature data show that GSK-3β plays a major function in WNT signalling pathway. The phosphorilation on Ser 9 inhibits the activity of Gsk-3β stimulating β-catenin nuclear translocation and enhancing β-catenin/TCF-mediated transcription. For this reason we then asked whether miR-34a overexpression influence the levels of Phospho-Gsk 3β (Ser9). Using Western blotting assays, we confirmed that, in SHEP Tr6 miR-34a#D, miR-34a overexpression also resulted in the inhibition of Phospho-Gsk 3β (Ser 9) levels. Total Gsk 3β was unchanged (Figure 24B). All together, these data indicate that the miR-34a led to WNT signaling down-regulation here investigated, thus confirming our predicted data. Here we comprehensively demonstrate the functional implication of miR-34a capabilities to simultaneously target components of several cancer signaling cascade, responsible for tumor progression.

2.4.3 Identification of late targets of miR-34a

In order to identify late targets of miR-34a, we analyzed the changes in protein expression levels induced by miR-34a 24 hours upon tetracycline stimulation and we found n.24 and n.29 proteins down-regulated respectively in SH-SY5Y in SHEP.

Among the 24 down-regulated proteins in SH-SY5Y cells, 9 had already been found down-regulated in previously analyzed time points (CATB, ANXA8, PLSL, GELS, CATD, SPRC, P4HA1, SODM, FKB10), indicating that still remain down-regulated, during miR-34a expression. Western blotting presented in figure 25 confirmed that SODM is already down regulated by miR-34a at 6 hours after induction and remains so even at 24 hours.
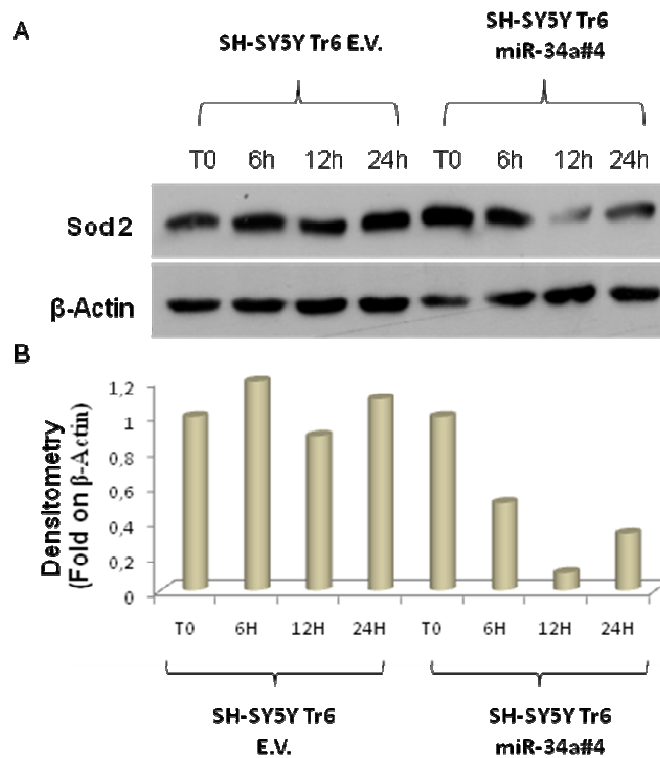
Figure 25. A. Total proteins prepared from SH-SY5Y Tr6 Empty vector (E.V.) or miR-34a overexpression (#4) treated with tetracycline for different time points (6hr, 12hr, 24hr) were subject to Western blotting anti-SODM antibody. β-Actin was used as loading control. **B.** Densiometric time-course analyses (Active β-Catenin), as β-Actin normalized. Data are means ±standard deviation of 3 experiments, each carried out in triplicate

Moreover, at this time point in SH-SY5Y has been identified new additional 15 proteins were found down-regulated. Searching in this protein set, for the presence of miR-34a seed-matching sequences in their 3' UTR transcripts, we noticed that miR-34a could potentially regulate the 3' UTR of 9 of these proteins (TBC13, RL1D1, MYO1B, GGA3, STAG2, TXTP, CCD56, DKC1, TPM1). While six proteins were annotated as not direct targets of miR-34a (SSXT, CC124, ALG5, ALDR, RET1, ULA1).

Regarding the proteins down-regulated in SHEP, we observed that 12 of 29 proteins were already found down-regulated at previously analyzed time points. Furthermore, 3 proteins (PLSL, CDC73, NOLC1) have been found down-regulated only after 24h in SHEP, while in SHSY already at 6 and 12 hours were inhibited by miR-34a, indicating that the silencing mechanisms, that regulate, at post transcriptionally level, the expression of these proteins in the two cellular systems are different. Additionally, we found 14 new down-regulated proteins, 12 of which had miR-34a seed-matching sequences in the 3' UTR of their transcripts (RRP1B, PA1B2, SPSY, FGF2, IMPA3, LRWD1, PAPS1, ERAP1, MP3B2, CT043, SRSF1, VP33B).

Here, we identified additional down-regulated proteins at early time point and some of them had putative miR-34a binding sites in their 3'UTR.

2.5 The regulation of protein expression by miR-34a is time depending

In our previous work we demonstrated that miR-34a doesn't exert its inhibitory effect on targets constantly during its expression. For example certain proteins, such as DLL1 and Cyclin D1, that were recognized as miR-34a targets, analyzed in a time dependent manner, showed fluctuation in their amount of protein quota, although the miRNA was continuously expressed [35]. So we asked whether there were other proteins in the proteome that do not show a constant expression pattern after miR-34a induction. The analyses performed above were carried out considering exclusively each time point. In order to compare each other the changes in protein expression at different times after miR-34a induction, the quantile normalization was applied. The quantile normalization generally is used to make two or more distribution identical in statistical properties [60,61].

Applying this technique, we obtained for each experiment (6h, 12 and 24 hours) a new normalized distributions, as shown by black curves in figure 26A and B (upper). Then, to calculate the upper and lower limit to define the regulated proteins (as described in the section 3.4), arithmetical mean between the new normalized mean (μ) was determined, as shown below:

1. SH-SY5Y

- SH-SY5Y 6h (Normalized μ_1)
- SH-SY5Y 12h (Normalized μ_2)
- SH-SY5Y 24h (Normalized μ_3)

Normalized mean (SH-SY5Y 6-12-24h) (μ_N)= (μ_1+ μ_2+ μ_3)/3= -0.34±0.27 (Figure XA)

2. SHEP

- SHEP 6h (Normalized μ_1)
- SHEP 12h (Normalized μ_2)
- SHEP 24h (Normalized μ_3)

Normalized mean (SHEP 6-12-24h) (μ_N)= (μ_1+ μ_2+ μ_3)/3= -0.01±0.32 (Figure 26B). Figure 26 shows the new normalized values of SHSY-5Y (A) and SHEP (B) cell experiments. The new values have the same distribution and can now be easily compared each other.
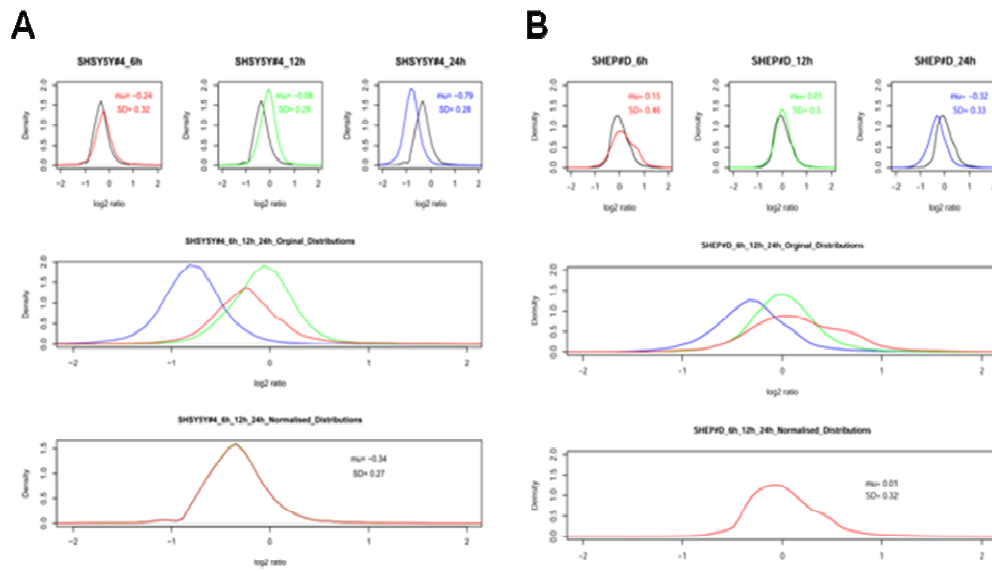
Figure 26 . To make the three distribution identical in statistical properties a quantile distribution was performed. The new normalized distribution of experiments performed in SH-SY5Y cells (A) was μ= -0.34±0.27, while in SHEP (B) was μ= -0.01±0.32.

After data normalization, we compared the differentially expressed proteins in each experiment and further statistical analyses were performed using Knime (Figure 27).

Figure 27 . Knime workflow showing the path followed to obtain the Lorenz curves and Gini coefficient for each protein.

51

To assess trend analysis of the proteins differentially expressed at different time points (6h, 12h and 24 hours), Lorenz curve and Gini coefficient were evaluated for each protein. 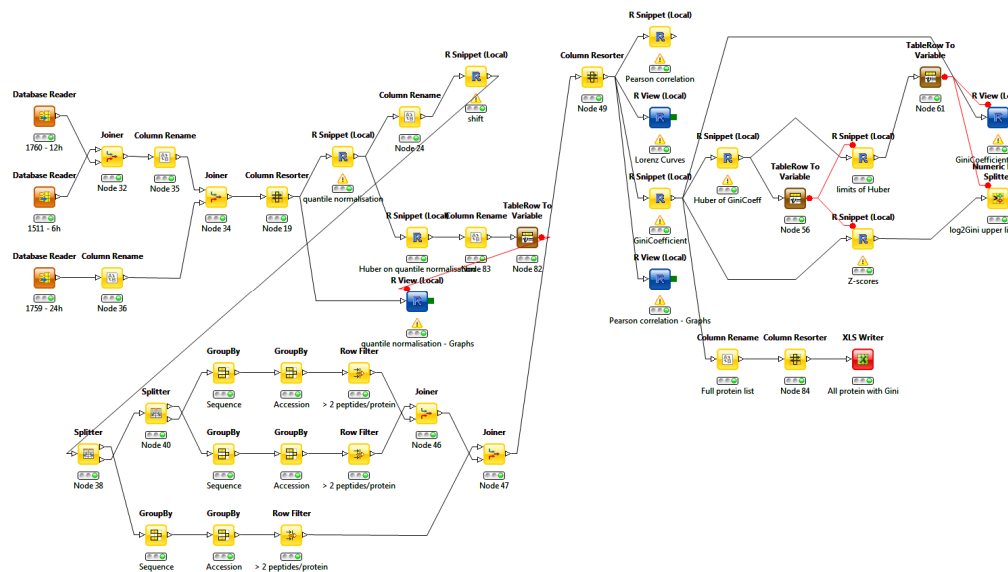The Lorenz curve is a graphical statistic that was first introduced in 1905 as a tool for exhibiting the concentration of wealth in a population (Lorenz MO, 1905). Originally were used to rank in terms of their wealth and the cumulative wealth, the members of the population (on the y-axis) against the cumulative proportion of the population (on the x-axis). One can then select any quantile to characterize concentration using a statistic such as 'Y per cent of the wealth is owned by X per cent of the population'.

Simply, The Lorenz Curve is a graphical representation of the proportionality of a distribution and represents a probability distribution of statistical values. Lorenz curve is often associated with income distribution calculations and commonly used in the analysis of inequality. Alternatively a summary index of concentration, the Gini coefficient (Gini C., 1914), is frequently used. In applications, the Gini coefficient frequently accompanies graphical presentation of the Lorenz curve. It is often used as a measure of income or wealth inequality. In brief, the Gini coefficient is usually defined mathematically based on the Lorenz curve, which plots the proportion of the total income of the population (y axis) that is cumulatively earned by the bottom x% of the population. The line at 45 degrees thus represents perfect equality of incomes.

Figure 28. Graphical representation of the Gini coefficient. The graph shows that the Gini coefficient is equal to the area marked A divided by the sum of the areas *A* and *B*. That is, Gini = A/(A+B). It is also equal to 2*A due to fact that A+B=0.5 (since the axes scale from 0 to 1).
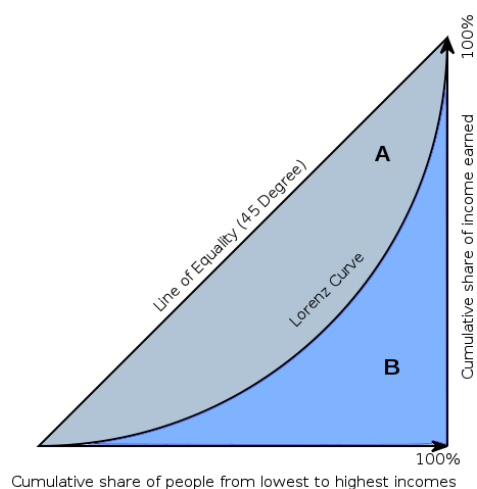
The Gini coefficient can then be thought of as the ratio of the area that lies between the line of equality and the Lorenz curve (marked *A* in the diagram) over the total area under the line of equality (marked *A* and *B* in the diagram); i.e.,G = *A* / (*A* + *B*) (Figure 28). A low Gini coefficient indicates a more equal distribution, with 0 corresponding to complete equality, while higher Gini coefficients indicate more unequal distribution, with 1 corresponding to complete inequality. Gini coefficient is a more complex calculation that allows us to assess the whether the changes, in protein expression level induced by miR34a over time, were significant. We evaluated the Lorenz curve for each protein of both cell line, as shown in figure 29 and the Gini coefficient, applying the formula reported in Materials and Methods section.
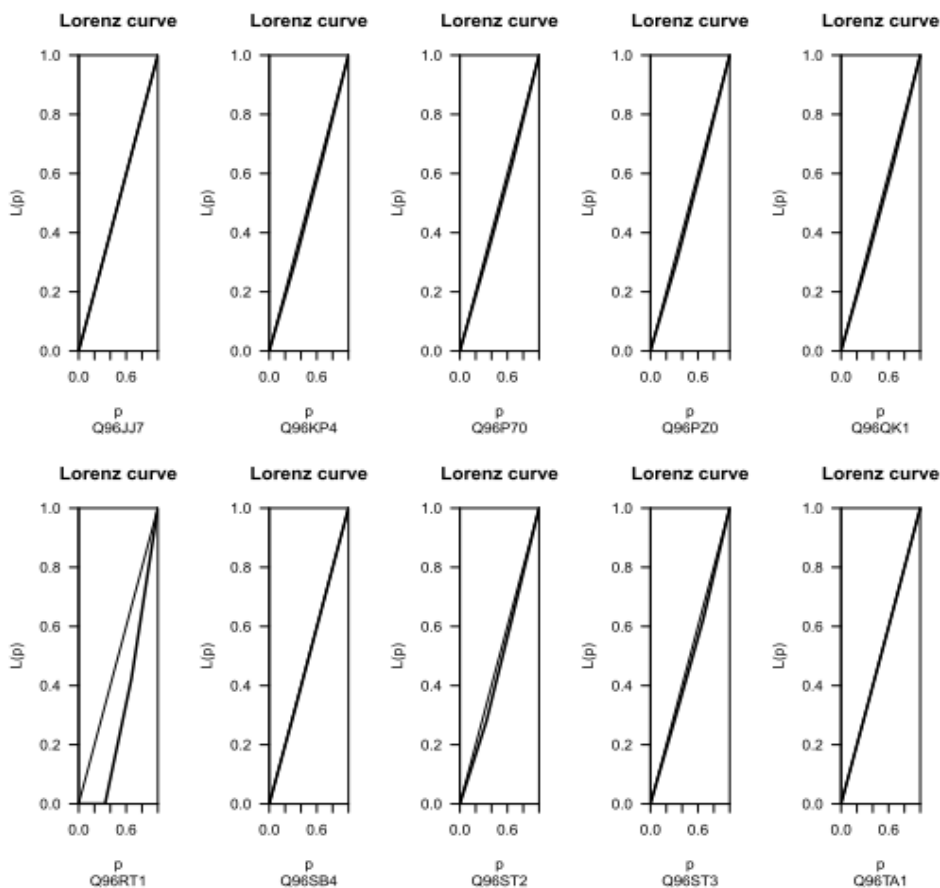
Figure 29. Lorenz curves of some representative proteins

Related to our experiments, a Gini coefficient equal to zero indicates that protein shows the same expression pattern at each time point. In this case the Lorenz curve overlaps the line of equality. While a Gini coefficient equal to one means that protein shows the same expression pattern during the analyzed time points; the Lorenz curve is far from the line of equality.

Figure 30. Expression levels of proteins dynamically regulated by miR-34a over the time in SH-SY5Y (A) and SHEP (B) cells. The values are expressed as log2 fold change.

To select the regulated proteins we used the upper limit of the Gini coefficient based on 99% of confidence interval. Our analyses revealed that in SHSY-5Y cells, among the 1331 detected proteins, 29 proteins did not show a constant expression pattern under time (Figure 30A). While in SHEP cells, 9 of 1067 detected proteins (Figure 30B) showed an oscillatory expression pattern.

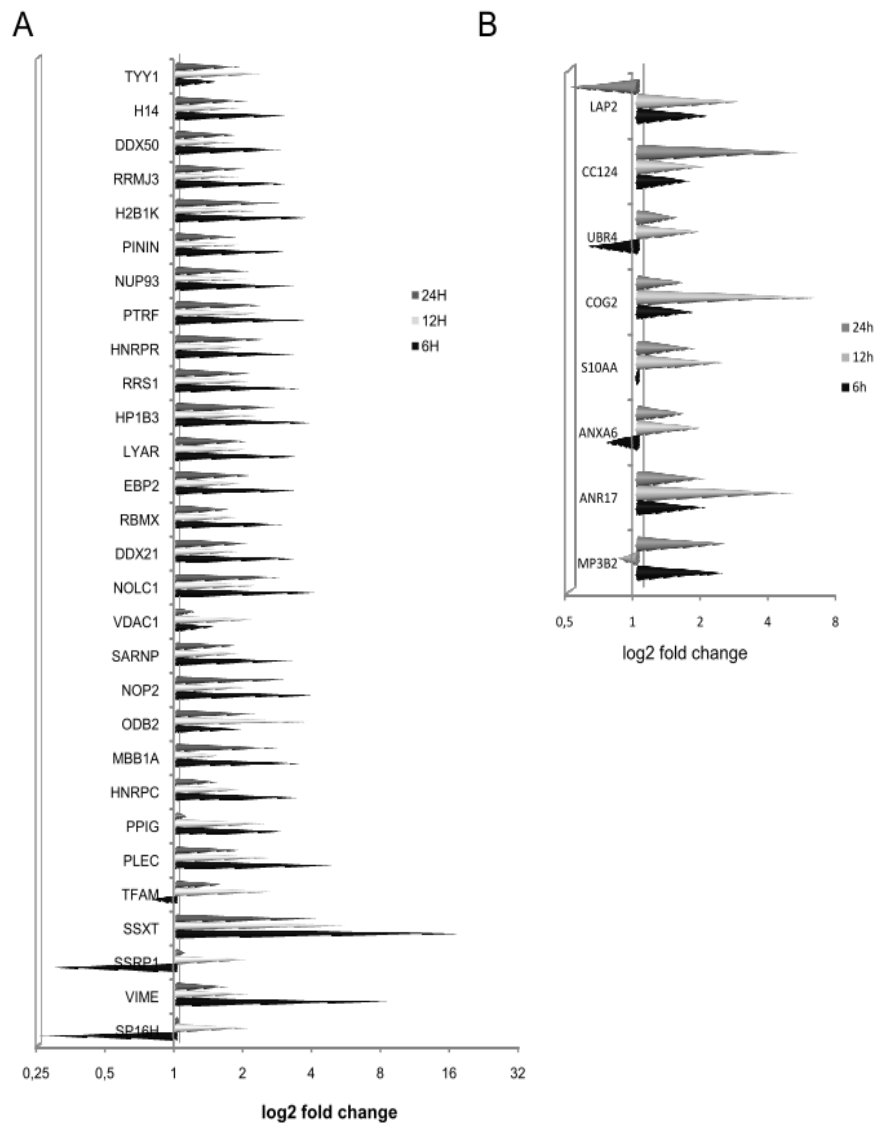Another graphical representation of the Gini coefficient is given by the scatter plots presented in figure 31. In these graphs were plotted the protein accession numbers (x-axis) versus Gini coefficient values (y-axis). The dotted line represent the threshold above which the proteins were considered dynamically regulated by miR-34a. Our analyses demonstrated that the effect of miR-34a down-regulation on this set of proteins, changes during the time.

This phenomenon may be due to different protein half-life within the cellular type, or the presence of other gene/protein factors that could regulate their expression as coactivators or repressors or by other mechanisms not yet here identified which need a further speculation and supporting data. Thus the finely controlled miR-34a machinery here identified regulates several new protein function as previously expected.
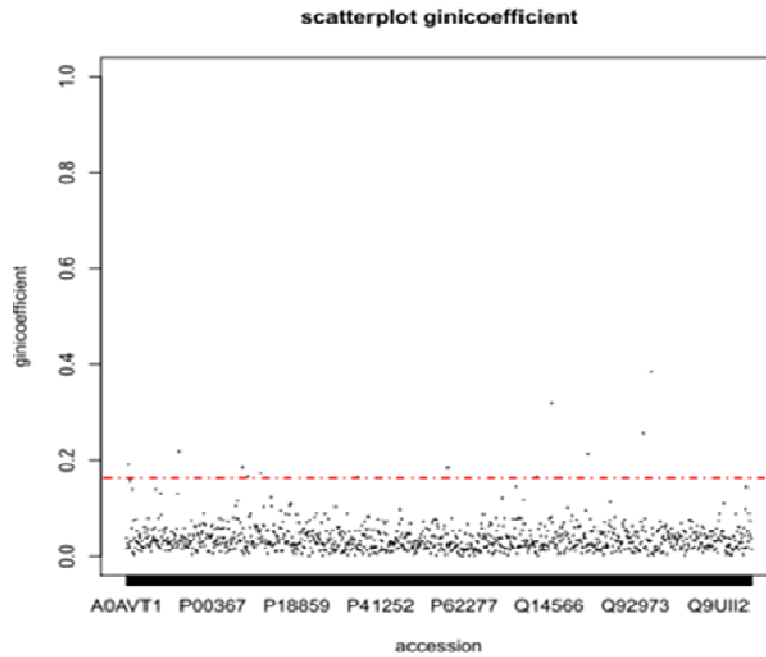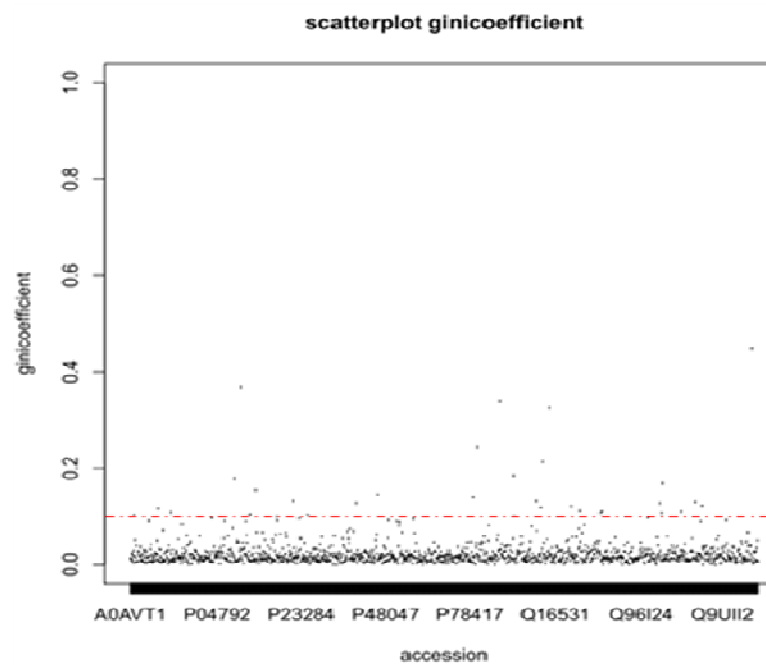
Figure 31. Scatter plots in which were plotted the protein accession numbers (x-axis) and Gini coefficient values (y-axis) of SHEP (A) and SY-SY5Y (B) cells. The dotted lines represent the threshold to define the proteins that were dynamically regulated.

2.5.1 More difference in protein expression at early time point

Having established that several proteins were regulated in a time-dependent manner, we began to investigate when the effects of miR-34a on protein expression are more pronounced.
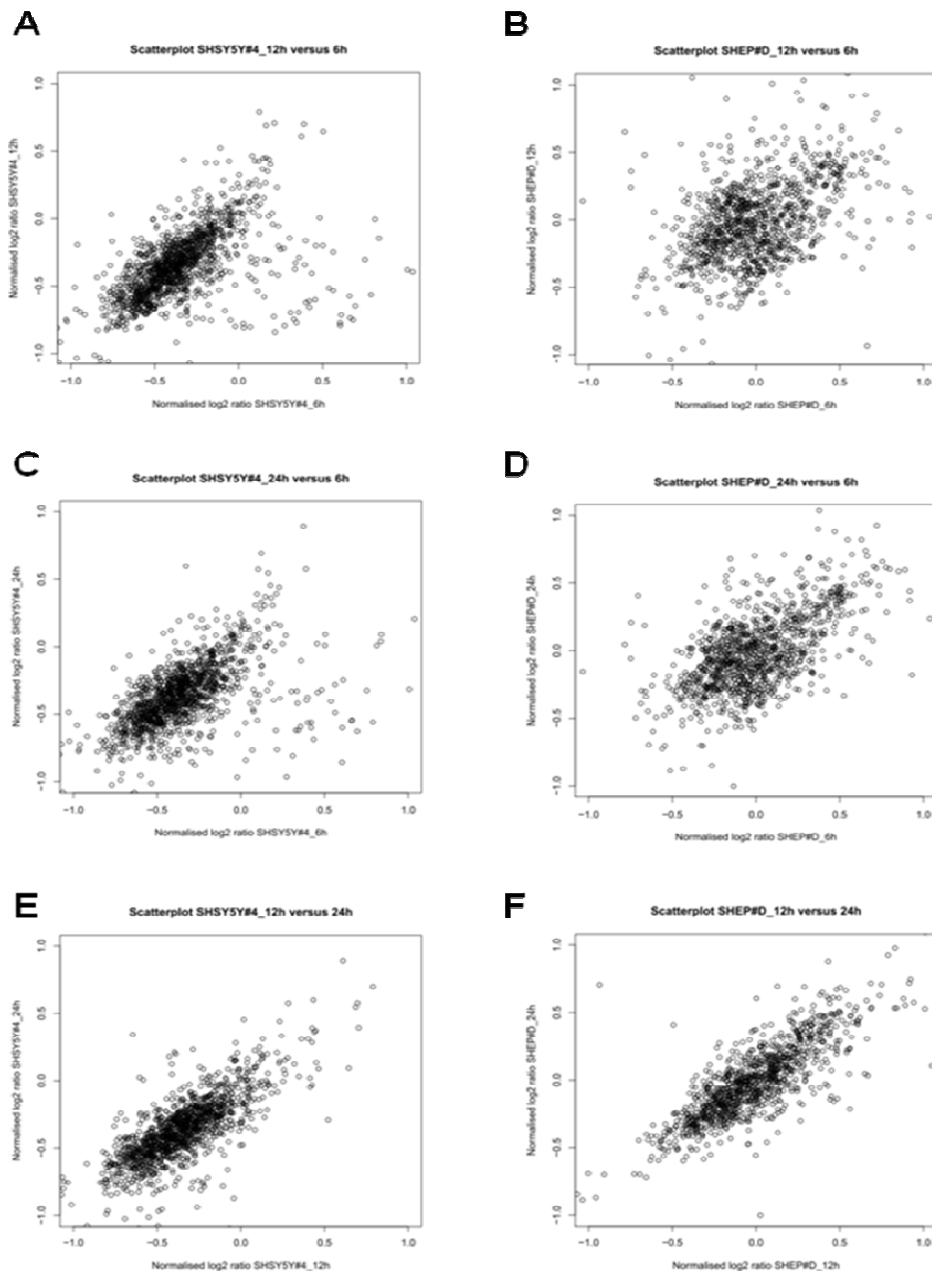
Figure 32. Scatter plots comparing protein expression changes between two time points. **A.B.** Scatter plots compare normalized log2 ratio of protein expression at 6 hr (x axis) against 12 hr (y axis) in SH-SY5Y (A) and SHEP (B) cells. **C.D.** Scatter plots compare normalized log2 ratio of protein expression at 6 hr (x axis) against 24 hr (y axis) in SH-SY5Y (C) and SHEP (D). **E.F.** Scatter plots compare normalized log2 ratio of protein expression at 12 hr (x axis) against 24 hr (y axis) in SH-SY5Y (E) and SHEP (F).

For this purpose we used the scatter plots graphical representation, to present measurements related to two variables.

Variables used in these graphs represent the fold change of protein expression in the same cellular system at two different time of miR-34a induction.

Scatter plots presented in figure 32, revealed that the magnitude of miR-34a effect on protein expression changes occurs at early time (6 hours) when compared to the later (12 and 24 hours) proteome output.

By analyzing normalized log2 ratio at 6h versus normalized log2 ratio at 12h or 24h the points spread showed higher then when were plotted log2 ratio at 12h versus normalized log2 ratio at 24h in both cells lines. All these data suggest that the magnitude of miR-34a effects on proteome occurs at early time after induction, upsetting all theories hitherto followed, according to which the effects on the proteome by a microRNA could be observed only after at least 24 hours.

Discussion 3

3. DISCUSSION

The emergence of shotgun proteomics has facilitated the numerous biological discoveries made by proteomic studies. However, comprehensive proteomic analysis remains challenging and shotgun proteomics is a continually changing field. The proteome is very dynamic and could mutate in response to cellular or environmental factors [62]. The identification of miRNA targets, functionally important in enhancing tumor capabilities, is crucial for understanding miRNA functions. By directly measuring changes in protein production, proteomic data are likely to be more relevant than microarray data. Moreover in silencing, operated by miRNA, not always were found correspondence between gene expression data and protein quota, this due to at least two different post-transcriptional regulations mechanism [63].

In this work we analyzed the proteome changes in two different NBL cell lines induced by ectopic expression of miR-34a. The analysis presented here revealed new direct targets of miR-34a, which presumably represent the mediator of its effects. The direct regulation by miR-34a was confirmed by reporter gene assays for selected miR-34a target mRNAs, showing that the miR-34a-mediated repression of these proteins requires the presence of seed-matching sequences in the respective 3'-UTRs.

Among the 2082 detected proteins, 172 were found significantly regulated, with 113 proteins being down- and 68 up-regulated. Perhaps surprisingly, the repressive effect on individual proteins wasn't relatively small and often exceeded fourfold, although we performed post-metabolic labeling. In effect, while in pulsed SILAC (pSILAC) method, only intensity differences between newly synthesized proteins (medium-heavy and heavy) are considered, in post-metabolic labeling there is the problem of persistence of stable proteins, that makes difficult to identify the down-regulation. This could also explain the reason for which we have not observed the change in protein expression of known miR-34a targets. Among the down-regulated proteins, we noted an overrepresentation of proteins involved in apoptosis, cell motility, cell division,

differentiation and mRNA processing. Even though the down-regulation of these proteins, which do not contain predicted miR-34a binding sites in their 3'-UTRs, presumably might be considered as secondary effect, following the direct miR-34a-mediated repression on other proteins that act upstream and regulate these functions, it reflects the cell cycle arrest and apoptosis as a major consequence of miR-34a activation.

In our analysis, we identified new targets of miR-34a (Table 3) and among these, seven proteins (LYAR, CTCF, TGM2, Ki67, TIMM13, ALG13 and ABCF2) have prognostic relevance in NBL. In fact, looking in a public database, we observed that all of these seven proteins correlate to bad clinical outcome when overexpressed in Neuroblastoma.

The newly identified miR-34a targets, LYAR, CTCF, TGM2, Ki67 and TIMM13 are linked to each other and together converge on important pathways involved in tumor progression, such as Wnt, TGF-β, Src/Fyn/Lyn, IGF and p53/myc as shown by the network in Figure 23.

Canonical Wnt signaling controls events ranging from cell fate determination and cell cycle regulation to cell motility and metabolism. In addition to the importance of the canonical Wnt pathway in normal cell function, pathologic increases in Wnt signaling are frequently implicated in neoplastic states. The importance of Wnt signaling in human cancer is highlighted by its coordinate control of the transcriptional programs underlying EMT, cancer stem cell generation and cancer progression. Wnt 1 has been previously been report to be a direct target of miR-34a [64] corroborating that miR-34a suppress oncogenic Wnt signaling.

Transforming Growth Factor β (TGF- β) was already found involved in signaling controls a diverse set of cellular processes, including cell proliferation, recognition, differentiation, apoptosis, and specification of developmental fate, during embryogenesis as well as in mature tissues, in species ranging from flies and worms to mammals [65-67]. TGF-β suppresses early-stage tumor development by virtue of its potent growth inhibitory effect,

but becomes a pro-oncogenic factor that stimulates tumor cell growth and invasiveness at later stages of tumorigenesis [68,69].

Pathological forms of TGFβ signaling promote tumor growth and invasion, evasion of immune surveillance, and cancer cell dissemination and metastasis. Moreover a recent study demonstrated the capability of miR-34a to target genes encoding multiple TGFβ isoforms [70]. The inhibition of these pathways by miR-34a was confirmed by literature and data obtained in our laboratory [71,72].

Another important corollary of our analysis here revealed, at the whole-proteome scale, the demonstration that the miR-34a effects on proteome occurs at early time point. *In-vitro* studies have already shown that miRNAs can induce translational inhibition in a very short time frame [73]. Therefore, the effects of miR-34a on proteome were investigated in a time-dependent manner, following time-courses in NBL cells at 6h, 12h and 24h after miR-34a induction. Our results demonstrated that miR-34a expression resulted in a regulation of protein expression more evident at 6 hours compared to other time points analyzed. At this time point, were found down-regulated 59 proteins in SH-SY5Y cells and 19 in SHEP. Some of these have seed sites in the 3'UTR of their transcripts that can explain the early down-regulation. A number of repressed proteins without seeds are nevertheless probably direct targets of the miR-34a. However, although some algorithms include searches for such sites, it seems that they could not identify these non-canonical sites with high success. Another explanation for these repressed proteins without seeds could be that are indirectly regulated by miR-34a and that, having a short half-life, it is possible to observe the down regulation also in such a short time. However we cannot exclude that the target genes that we tested for which we did not find miR-34a seed match in the 3'UTR might be direct targets, regulated by sequences in the 5'UTR or CDS.

It is also worth noting that, our data further showed the kinetics of miR-34a regulation analyzing here, for the first time the effects of miR-34a on proteome

in a time-dependent manner, allowing us to obtain a global picture of miR-34a functions. These data provides a clear and effective answer to the long-standing question on when miRNA acts on their targets and this is in stark contrast to literature data in which miRNA inhibitory effects were evaluated at later time point.

Finally, we observed that the down-regulation of several proteins is maintained even in later times, but some proteins were found dynamically regulated over time. It is conceivable that such proteins, given the complexity of the system here analyzed, belong to key group of proteins, whose expression was finely controlled. Thus strengthening our hypothesis that observing the effects of micro RNA at a single time point could result in the loss of the identification of many target.

Recently, *in vivo* studies showed that tumor growth was significantly repressed after exogenous miR-34a administration in retroperitoneal Neuroblastoma tumors [74]. Identification of miR-34a as is a highly significant finding with respect to the development of potential therapeutics for this disease. Current therapies for high risk Neuroblastoma include chemo- and radiation-therapy in an attempt to hinder tumor relapse.

Therefore, ectopic miR-34a expression may serve as a tumor therapeutic means for human tumors in the future. A comprehensive knowledge of the targets and effects of miR-34a is of relevance in order to evaluate the potential side effects of such therapies. The study presented here is an important step in the direction of obtaining a complete picture of miR-34a targets. In the future, analysis of up-regulated proteins may facilitate a more complete coverage of miRNA targets.

Conclusions 4

4. Conclusions

The role of miRNAs in mediating critical cellular processes is an emerging field in cancer genetics. Dysregulation, enhanced expression and selective inhibition of miRNAs has improved scientific understanding of the functional role which these regulatory molecules play in cancer progression and patient prognosis. MiR-34a was the first miRNA identified as a putative tumor suppressor in Neuroblastoma through its direct targeting of transcription factors and other genes essential for cellular proliferation. Here, we identify new early targets of miR-34a, adding an important step in understanding the mechanisms of action of this microRNA. Although miRNAs are largely known to repressively regulate protein expression, it has been reported that some miRNAs can also upregulate translation [75]. In this study, we focused on the repressive gene regulation of the miRNAs as a result of their binding to the 3'UTR of target genes, and identified only proteins that were downregulated by miR-34a, although many upregulated proteins were also detected by quantitative bottom-up proteomics analysis. Further experiments will be needed to determine how, mechanistically, miR-34a was able to upregulate these proteins. The cell clones here analyzed are now ready for a second level of analyses verifying how miR-34a would influence the expression of other miRNAs coupled to Long non coding RNAs and how altogether in a complexity network of action contribute to NBL progression. These results will be issue of future efforts.

In conclusion, in this work our effort was oriented not only to identify new targets of miR-34a in Neuroblastoma, but also to show that the kinetics of regulation of a micro RNA can be very fast and dynamic.

Novelties

In this thesis, we identified new targets of miR-34a, some of them with a prognostic relevance in NBL. In fact, looking in a public database, we observed that these proteins correlate to bad clinical outcome when overexpressed in Neuroblastoma. It would be interesting to study the effects of such down-regulation given that little is known about the function of these proteins in Neuroblastoma,

Our study also demonstrated that the miR-34a effects on proteome occurs at early time point and that the down-regulation of several proteins is maintained even in later times. However some proteins were found dynamically regulated by mir-34a over time. These data are important because they open the way to a better understanding on the timing and mechanisms of action of a microRNA.

Materials and Methods 5

5. Materials and Methods

Cell culture

The Neuroblastoma cell lines SHEP and SH-SY5Y were kept in RPMI medium containing 10% (v/v) fetal calf serum, 2 mM L-glutamine, and 1% pen/strep. Cells were transfected with the pcDNA™6/TR plasmid, which encodes Tet repressor (TetR) using Lipofectamine2000 (Invitrogen). Polyclonal cell pools were generated by selection with blasticidin (5 µg/ml) for 10 days. Positive clones were transfected with the episomal pT-REx-DEST vector encoding miR-34a. Polyclonal cell pools were generated by selection with hygromycin (500 µg/ml). The percentage of Tr6/ pT-REx-DEST miR-34a-positive cells was determined 12 h after addition of tetracycline at a final concentration of 2 µg/ml.

RNA extraction and Quantitative Real Time PCR

Total RNA was extracted from cells using Trizol reagent [Invitrogen] according to manufacturer's recommendations and were treated with RNase free DNase [Promega]. Total RNA [1 µg] was reverse transcribed using iScript™ cDNA Syntesis Kit [Biorad]. The RT products [cDNA] were amplified by real-time quantitative PCR using 7900 Real-Time PCR System [Applied Biosystems, Foster City; CA] with Power SYBR green Master Mix.

For all SYBR Green PCR, Ct values were normalized to either U6. Relative expressions of target genes were determined by the $2^{-\Delta\Delta Ct}$ method. All of the data are presented as means ± standard error of two to three replicate experiments.

Western blotting

Cells were washed in cold phosphate-buffered saline and lysed in protein lysis buffer (20 mM sodium phosphate, pH 7.4, 150 mM NaCl, 10% glycerol, 1% Na-deoxycholate and 1% Triton X-100) supplemented with protease inhibitors

(Roche). Cell lysates (50 µg) were electrophoresed on 10% SDS-PAGE gels and transferred onto PVDF membranes (Millipore). After 1 hour blocking with 5% dry milk fat in phosphate-buffered saline containing 0.02% Tween-20, the membranes were incubated with the primary antibody overnight at 4 °C, and with the secondary antibody for 1 h at room temperature. The bands were visualized with a chemiluminescence detection system (Pierce), according to the manufacturer instructions.

Shotgun analysis with differential labeling

To analyze the impact of mir34a activation on protein output we used the post-metabolic labelling (propionylation) with NHS-propionylate (C_{12} and C_{13}) on Lysine (K) and Arginine (R) residues coupled with mass spectrometry analysis, as described above [76]. In breaf, each sample was first desalted by loading 1 ml of sample on a NAP^{TM}-5 column Sephadex^{TM}-G25 DNA Grade [GE Healthcare] and then digested by adding trypsin in a trypsin/protein ratio of 1/50 and incubating overnight at 37 °C. To synthesize isotopically labeled reagents NHS-propionate (3 C_{12}) and NHS-propionate (3 C_{13}) was used. Once the samples were labelled, a quick analysis, based on 10 light and heavy peptide couples, on the Q-tof Premier was performed to determine the 1:1 mixing of the labelled samples. The samples were mixed together in a 1:1 ratio and were fractionated on a RP-HPLC. After the fractionation, fractions with a difference of 20 minutes were pooled together to reduce the number of mass spectrometry samples.

Knime: The Konstanz Information Miner

To manipulate the large data set obtain the protein lists, we used Knime. To The need for modular data analysis environments has increased dramatically over the past years. In order to make use of the vast variety of data analysis methods around, it is essential that such an environment is easy and intuitive to

use, allows for quick and interactive changes to the analysis and enables the user to visually explore the results.

To meet these challenges a data pipelining environment is an appropriate model. It allows the user to visually assemble and adapt the analysis flow from standardized building blocks, at the same time offering an intuitive, graphical way to document what has been done. Knime, the Konstanz Information Miner provides such an environment.

The Konstanz Information Miner is a modular environment which enables easy visual assembly and interactive execution of a data pipeline. It is designed as a teaching, research and collaboration platform, which enables easy integration of new algorithms, data manipulation or visualization methods as new modules or nodes.

MiR 34a target prediction

MiR-34a targets were selected by examining predicted targets from TargetScan, miRanda, and PITA. Each database relies on different algorithms of target prediction and uses different read-out scales. Potential gene targets were chosen based on the presence in at least two of all of the predicted algorithms used in the analyses.

Cloning of 3' UTRs

The 3' UTRs of the indicated target mRNAs containing putative miR-34a binding sites were PCR-amplified from human genomic DNA with the Kapa HiFi Hot start (Kapa Biosystem). The 3' UTRs were cloned into pGL3-control-MCS and verified by sequencing.

Luciferase Assays

HEK293 cells were seeded in 12-well format and transfected after 48 hours with 100 ng of the indicated firefly luciferase reporter plasmid, 20 ng of Renilla reporter plasmid as a normalization control, and 25 ng of miR-34a or a

negative control oligonucleotide. Luciferase assays were carried out following 24 hours of transfection using the Dual Luciferase Reporter assay system (Promega) according to manufacturer's instructions. Fluorescence intensities were measured with a luminometer (Berthold).

Inequality Measurements

Fluctuation in protein expression during the time was measured applying the Gini's method, which has been commonly used in the economics and social science [18–20]. One of the basic measures of the Gini's method is the Gini coefficient (also known as Gini index), which has been well defined for quantifying variable inequalities in a population. For a given variable X, the Gini coefficient can be computed with the formula [21]

$$G = (\Sigma^n_{i=1}(2i-n-1)X_{(i)}) / (n-1) \Sigma^n_{i=1} X_{(i)}$$

where n (n $\geq$ 2) is the number of considered variable in the population, and X (i) is the ith value of considered variable sorted in increasing order, $0 \leq X_{(1)} \leq X_{(2)} \leq \cdots \leq X_{(n)}$.

The Gini coefficient can be ranged from 0.0 (complete equality) to 1.0 (complete or absolute inequality). In our experiments a Gini coefficient equal to zero indicates that protein shows the same expression pattern at each time point, while a Gini coefficient equal to one means that protein shows the same expression pattern during the analyzed time points

Statistical Analyses

All biochemical experiments were done in triplicate unless otherwise stated. Two-tailed Student's t test was used to test significance. Survival curves were constructed by the Kaplan and Meier method, with differences between curves tested for statistical significance using the log-rank test.

References

References

1. Schwab M, Westermann F, Hero B, Berthold F (2003) Neuroblastoma: biology and molecular and chromosomal pathology. Lancet Oncol 4: 472-480.

2. Brodeur GM (2003) Neuroblastoma: biological insights into a clinical enigma. Nat Rev Cancer 3: 203-216.

3. Cohn SL, Pearson AD, London WB, Monclair T, Ambros PF, et al. (2009) The International Neuroblastoma Risk Group (INRG) classification system: an INRG Task Force report. J Clin Oncol 27: 289-297.

4. Monclair T, Brodeur GM, Ambros PF, Brisse HJ, Cecchetto G, et al. (2009) The International Neuroblastoma Risk Group (INRG) staging system: an INRG Task Force report. J Clin Oncol 27: 298-303.

5. Ambros PF, Ambros IM, Brodeur GM, Haber M, Khan J, et al. (2009) International consensus for neuroblastoma molecular diagnostics: report from the International Neuroblastoma Risk Group (INRG) Biology Committee. Br J Cancer 100: 1471-1482.

6. Bagatell R, Rumcheva P, London WB, Cohn SL, Look AT, et al. (2005) Outcomes of children with intermediate-risk neuroblastoma after treatment stratified by MYCN status and tumor cell ploidy. J Clin Oncol 23: 8819-8827.

7. George RE, London WB, Cohn SL, Maris JM, Kretschmar C, et al. (2005) Hyperdiploidy plus nonamplified MYCN confers a favorable prognosis in children 12 to 18 months old with disseminated neuroblastoma: a Pediatric Oncology Group study. J Clin Oncol 23: 6466-6473.

8. Look AT, Hayes FA, Shuster JJ, Douglass EC, Castleberry RP, et al. (1991) Clinical relevance of tumor cell ploidy and N-myc gene amplification in childhood neuroblastoma: a Pediatric Oncology Group study. J Clin Oncol 9: 581-591.

9. Weiss WA, Aldape K, Mohapatra G, Feuerstein BG, Bishop JM (1997) Targeted expression of MYCN causes neuroblastoma in transgenic mice. EMBO J 16: 2985-2995.

10. Brodeur GM, Seeger RC, Schwab M, Varmus HE, Bishop JM (1984) Amplification of N-myc in untreated human neuroblastomas correlates with advanced disease stage. Science 224: 1121-1124.

11. Seeger RC, Brodeur GM, Sather H, Dalton A, Siegel SE, et al. (1985) Association of multiple copies of the N-myc oncogene with rapid progression of neuroblastomas. N Engl J Med 313: 1111-1116.

12. Westermann F, Muth D, Benner A, Bauer T, Henrich KO, et al. (2008) Distinct transcriptional MYCN/c-MYC activities are associated with spontaneous regression or malignant progression in neuroblastomas. Genome Biol 9: R150.

13. Breen CJ, O'Meara A, McDermott M, Mullarkey M, Stallings RL (2000) Coordinate deletion of chromosome 3p and 11q in neuroblastoma detected by comparative genomic hybridization. Cancer Genet Cytogenet 120: 44-49.

14. Ejeskar K, Aburatani H, Abrahamsson J, Kogner P, Martinsson T (1998) Loss of heterozygosity of 3p markers in neuroblastoma tumours implicate a tumour-suppressor locus distal to the FHIT gene. Br J Cancer 77: 1787-1791.

15. Luttikhuis ME, Powell JE, Rees SA, Genus T, Chughtai S, et al. (2001) Neuroblastomas with chromosome 11q loss and single copy MYCN comprise a biologically distinct group of tumours with adverse prognosis. Br J Cancer 85: 531-537.

16. Plantaz D, Vandesompele J, Van Roy N, Lastowska M, Bown N, et al. (2001) Comparative genomic hybridization (CGH) analysis of stage 4 neuroblastoma reveals high frequency of 11q deletion in tumors lacking MYCN amplification. Int J Cancer 91: 680-686.

17. Hoebeeck J, Michels E, Menten B, Van Roy N, Eggert A, et al. (2007) High resolution tiling-path BAC array deletion mapping suggests commonly involved 3p21-p22 tumor suppressor genes in neuroblastoma and more frequent tumors. Int J Cancer 120: 533-538.

18. Attiyeh EF, London WB, Mosse YP, Wang Q, Winter C, et al. (2005) Chromosome 1p and 11q deletions and outcome in neuroblastoma. N Engl J Med 353: 2243-2253.

19. McArdle L, McDermott M, Purcell R, Grehan D, O'Meara A, et al. (2004) Oligonucleotide microarray analysis of gene expression in neuroblastoma displaying loss of chromosome 11q. Carcinogenesis 25: 1599-1609.

20. Ando K, Ohira M, Ozaki T, Nakagawa A, Akazawa K, et al. (2008) Expression of TSLC1, a candidate tumor suppressor gene mapped to chromosome 11q23, is downregulated in unfavorable neuroblastoma without promoter hypermethylation. Int J Cancer 123: 2087-2094.

21. Michels E, Hoebeeck J, De Preter K, Schramm A, Brichard B, et al. (2008) CADM1 is a strong neuroblastoma candidate gene that maps within a 3.72 Mb critical region of loss on 11q23. BMC Cancer 8: 173.

22. Nowacki S, Skowron M, Oberthuer A, Fagin A, Voth H, et al. (2008) Expression of the tumour suppressor gene CADM1 is associated with favourable outcome and inhibits cell survival in neuroblastoma. Oncogene 27: 3329-3338.

23. Van Roy N, Laureys G, Cheng NC, Willem P, Opdenakker G, et al. (1994) 1;17 translocations and other chromosome 17 rearrangements in human primary neuroblastoma tumors and cell lines. Genes Chromosomes Cancer 10: 103-114.

24. Savelyeva L, Corvi R, Schwab M (1994) Translocation involving 1p and 17q is a recurrent genetic alteration of human neuroblastoma cells. Am J Hum Genet 55: 334-340.

25. Vandepoele K, Andries V, Van Roy N, Staes K, Vandesompele J, et al. (2008) A constitutional translocation t(1;17)(p36.2;q11.2) in a neuroblastoma patient disrupts the human NBPF1 and ACCN1 genes. PLoS One 3: e2207.

26. Garzia L, Andolfo I, Cusanelli E, Marino N, Petrosino G, et al. (2009) MicroRNA-199b-5p impairs cancer stem cells through negative regulation of HES1 in medulloblastoma. PLoS ONE 4: e4998.

27. Lodygin D, Tarasov V, Epanchintsev A, Berking C, Knyazeva T, et al. (2008) Inactivation of miR-34a by aberrant CpG methylation in multiple types of cancer. Cell Cycle 7: 2591-2600.

28. He L, He X, Lim LP, de Stanchina E, Xuan Z, et al. (2007) A microRNA component of the p53 tumour suppressor network. Nature 447: 1130-1134.

29. Raver-Shapira N, Marciano E, Meiri E, Spector Y, Rosenfeld N, et al. (2007) Transcriptional activation of miR-34a contributes to p53-mediated apoptosis. Mol Cell 26: 731-743.

30. Bommer GT, Gerin I, Feng Y, Kaczorowski AJ, Kuick R, et al. (2007) p53-mediated activation of miRNA34 candidate tumor-suppressor genes. Curr Biol 17: 1298-1307.

31. Dutta KK, Zhong Y, Liu YT, Yamada T, Akatsuka S, et al. (2007) Association of microRNA-34a overexpression with proliferation is cell type-dependent. Cancer Sci 98: 1845-1852.

32. Chen Y, Stallings RL (2007) Differential patterns of microRNA expression in neuroblastoma are correlated with prognosis, differentiation, and apoptosis. Cancer Res 67: 976-983.

33. Chang TC, Yu D, Lee YS, Wentzel EA, Arking DE, et al. (2008) Widespread microRNA repression by Myc contributes to tumorigenesis. Nat Genet 40: 43-50.

34. Fontana L, Fiori ME, Albini S, Cifaldi L, Giovinazzi S, et al. (2008) Antagomir-17-5p abolishes the growth of therapy-resistant neuroblastoma through p21 and BIM. PLoS One 3: e2236.

35. de Antonellis P, Medaglia C, Cusanelli E, Andolfo I, Liguori L, et al. (2011) MiR-34a targeting of Notch ligand delta-like 1 impairs CD15+/CD133+ tumor-propagating cells and supports neural differentiation in medulloblastoma. PLoS One 6: e24584.

36. Hermeking H (2010) The miR-34 family in cancer and apoptosis. Cell Death Differ 17: 193-199.

37. Sonnenberg A, Liem RK (2007) Plakins in development and disease. Exp Cell Res 313: 2189-2203.

38. Leung CL, Green KJ, Liem RK (2002) Plakins: a family of versatile cytolinker proteins. Trends Cell Biol 12: 37-45.

39. Bausch D, Thomas S, Mino-Kenudson M, Fernandez-del CC, Bauer TW, et al. (2011) Plectin-1 as a novel biomarker for pancreatic cancer. Clin Cancer Res 17: 302-309.

40. Litjens SH, de Pereda JM, Sonnenberg A (2006) Current insights into the formation and breakdown of hemidesmosomes. Trends Cell Biol 16: 376-383.

41. Guha U, Chaerkady R, Marimuthu A, Patterson AS, Kashyap MK, et al. (2008) Comparisons of tyrosine phosphorylated proteins in cells expressing lung cancer-specific alleles of EGFR and KRAS. Proc Natl Acad Sci U S A 105: 14112-14117.

42. Morello LG, Coltri PP, Quaresma AJ, Simabuco FM, Silva TC, et al. (2011) The human nucleolar protein FTSJ3 associates with NIP7 and functions in pre-rRNA processing. PLoS One 6: e29174.

43. Kertesz M, Iovino N, Unnerstall U, Gaul U, Segal E (2007) The role of site accessibility in microRNA target recognition. Nat Genet 39: 1278-1284.

44. Su L, Hershberger RJ, Weissman IL (1993) LYAR, a novel nucleolar protein with zinc finger DNA-binding motifs, is involved in cell growth regulation. Genes Dev 7: 735-748.

45. Cai J, Chen J, Liu Y, Miura T, Luo Y, et al. (2006) Assessing self-renewal and differentiation in human embryonic stem cell lines. Stem Cells 24: 516-530.

46. Li H, Wang B, Yang A, Lu R, Wang W, et al. (2009) Ly-1 antibody reactive clone is an important nucleolar protein for control of self-renewal and differentiation in embryonic stem cells. Stem Cells 27: 1244-1254.

47. Docquier F, Farrar D, D'Arcy V, Chernukhin I, Robinson AF, et al. (2005) Heightened expression of CTCF in breast cancer cells is associated with resistance to apoptosis. Cancer Res 65: 5112-5122.

48. Fiorentino FP, Macaluso M, Miranda F, Montanari M, Russo A, et al. (2011) CTCF and BORIS regulate Rb2/p130 gene transcription: a novel mechanism and a new paradigm for understanding the biology of lung cancer. Mol Cancer Res 9: 225-233.

49. Torrano V, Chernukhin I, Docquier F, D'Arcy V, Leon J, et al. (2005) CTCF regulates growth and erythroid differentiation of human myeloid leukemia cells. J Biol Chem 280: 28152-28161.

50. Qi CF, Martensson A, Mattioli M, Dalla-Favera R, Lobanenkov VV, et al. (2003) CTCF functions as a critical regulator of cell-cycle arrest and death after ligation of the B cell receptor on immature B cells. Proc Natl Acad Sci U S A 100: 633-638.

51. Heath H, Ribeiro de Almeida C, Sleutels F, Dingjan G, van de Nobelen S, et al. (2008) CTCF regulates cell cycle progression of alphabeta T cells in the thymus. EMBO J 27: 2839-2850.

52. Mann AP, Verma A, Sethi G, Manavathi B, Wang H, et al. (2006) Overexpression of tissue transglutaminase leads to constitutive

activation of nuclear factor-kappaB in cancer cells: delineation of a novel pathway. Cancer Res 66: 8788-8795.

53. Mangala LS, Fok JY, Zorrilla-Calancha IR, Verma A, Mehta K (2007) Tissue transglutaminase expression promotes cell attachment, invasion and survival in breast cancer cells. Oncogene 26: 2459-2470.

54. Miyoshi N, Ishii H, Mimori K, Tanaka F, Hitora T, et al. (2010) TGM2 is a novel marker for prognosis and therapeutic target in colorectal cancer. Ann Surg Oncol 17: 967-972.

55. Cao L, Shao M, Schilder J, Guise T, Mohammad KS, et al. (2012) Tissue transglutaminase links TGF-beta, epithelial to mesenchymal transition and a stem cell phenotype in ovarian cancer. Oncogene 31: 2521-2534.

56. Ogawa Y, Tsuda H, Hai E, Tsuji N, Yamagata S, et al. (2006) Clinical role of ABCF2 expression in breast cancer. Anticancer Res 26: 1809-1814.

57. Tsuda H, Ito YM, Ohashi Y, Wong KK, Hashiguchi Y, et al. (2005) Identification of overexpression and amplification of ABCF2 in clear cell ovarian adenocarcinomas by cDNA microarray analyses. Clin Cancer Res 11: 6880-6888.

58. Gong P, Wang Y, Liu G, Zhang J, Wang Z (2013) New insight into ki67 expression at the invasive front in breast cancer. PLoS One 8: e54912.

59. Lutz T, Neupert W, Herrmann JM (2003) Import of small Tim proteins into the mitochondrial intermembrane space. EMBO J 22: 4400-4408.

60. Callister SJ, Barry RC, Adkins JN, Johnson ET, Qian WJ, et al. (2006) Normalization approaches for removing systematic biases associated with mass spectrometry and label-free proteomics. J Proteome Res 5: 277-286.

61. Bolstad BM, Irizarry RA, Astrand M, Speed TP (2003) A comparison of normalization methods for high density oligonucleotide array data based on variance and bias. Bioinformatics 19: 185-193.

62. Gilmore JM, Washburn MP (2010) Advances in shotgun proteomics and the analysis of membrane proteomes. J Proteomics 73: 2078-2091.

63. Bartel DP (2004) MicroRNAs: genomics, biogenesis, mechanism, and function. Cell 116: 281-297.

64. Hashimi ST, Fulcher JA, Chang MH, Gov L, Wang S, et al. (2009) MicroRNA profiling identifies miR-34a and miR-21 and their target genes JAG1 and WNT1 in the coordinate regulation of dendritic cell differentiation. Blood 114: 404-414.

65. Patterson GI, Padgett RW (2000) TGF beta-related pathways. Roles in Caenorhabditis elegans development. Trends Genet 16: 27-33.

66. Massague J, Blain SW, Lo RS (2000) TGFbeta signaling in growth control, cancer, and heritable disorders. Cell 103: 295-309.

67. Massague J (2000) How cells read TGF-beta signals. Nat Rev Mol Cell Biol 1: 169-178.

68. Massague J (2008) TGFbeta in Cancer. Cell 134: 215-230.

69. Javelaud D, Alexaki VI, Mauviel A (2008) Transforming growth factor-beta in cutaneous melanoma. Pigment Cell Melanoma Res 21: 123-132.

70. Lal A, Thomas MP, Altschuler G, Navarro F, O'Day E, et al. (2011) Capture of microRNA-bound mRNAs identifies the tumor suppressor miR-34a as a regulator of growth factor signaling. PLoS Genet 7: e1002363.

71. Yang P, Li QJ, Feng Y, Zhang Y, Markowitz GJ, et al. (2012) TGF-beta-miR-34a-CCL22 signaling-induced Treg cell recruitment promotes venous metastases of HBV-positive hepatocellular carcinoma. Cancer Cell 22: 291-303.

72. Genovese G, Ergun A, Shukla SA, Campos B, Hanna J, et al. (2012) microRNA regulatory network inference identifies miR-34a as a novel regulator of TGF-beta signaling in glioblastoma. Cancer Discov 2: 736-749.

73. Mathonnet G, Fabian MR, Svitkin YV, Parsyan A, Huck L, et al. (2007) MicroRNA inhibition of translation initiation in vitro by targeting the cap-binding complex eIF4F. Science 317: 1764-1767.

74. Tivnan A, Tracey L, Buckley PG, Alcock LC, Davidoff AM, et al. (2011) MicroRNA-34a is a potent tumor suppressor molecule in vivo in neuroblastoma. BMC Cancer 11: 33.

75. Vasudevan S, Tong Y, Steitz JA (2007) Switching from repression to activation: microRNAs can up-regulate translation. Science 318: 1931-1934.

76. Staes A, Impens F, Van Damme P, Ruttens B, Goethals M, et al. (2011) Selecting protein N-terminal peptides by combined fractional diagonal chromatography. Nat Protoc 6: 1130-1141.

Publications

Neuroblastoma tumorigenesis is regulated through the Nm23-H1/h-Prune C-terminal interaction.

Carotenuto M, Pedone E, Diana D, de Antonellis P, Džeroski S, Marino N, Navas L, Di Dato V, Scoppettuolo MN, Cimmino F, Correale S, Pirone L, Monti SM, Bruder E, Zenko B, Slavkov I, Pastorino F, Ponzoni M, Schulte JH, Schramm A, Eggert A, Westermann F, Arrigoni G, Accordi B, Basso G, Saviano M, Fattorusso R, Zollo M.
Sci Rep. 2013 Mar 1;3:1351.

MicroRNA 199b-5p delivery through stable nucleic acid lipid particles (SNALPs) in tumorigenic cell lines.

de Antonellis P, Liguori L, Falanga A, Carotenuto M, Ferrucci V, Andolfo I, Marinaro F, Scognamiglio I, Virgilio A, De Rosa G, Galeone A, Galdiero S, Zollo M.
Naunyn Schmiedebergs Arch Pharmacol. 2013 Apr;386(4):287-302.

MiR-34a targeting of Notch ligand delta-like 1 impairs CD15+/CD133+ tumor-propagating cells and supports neural differentiation in medulloblastoma.

de Antonellis P, Medaglia C, Cusanelli E, Andolfo I, Liguori L, De Vita G, Carotenuto M, Bello A, Formiggini F, Galeone A, De Rosa G, Virgilio A, Scognamiglio I, Sciro M, Basso G, Schulte JH, Cinalli G, Iolascon A, Zollo M.
PLoS One. 2011;6(9):e24584.

Norcantharidin impairs medulloblastoma growth by inhibition of Wnt/β-catenin signaling.

Cimmino F, Scoppettuolo MN, Carotenuto M, De Antonellis P, Dato VD, De Vita G, Zollo M. J Neurooncol. 2012 Jan;106(1):59-70.

Acknowledgments

Acknowledgments

I would like to thank my tutor Prof. Massimo Zollo for giving me the opportunity to work in his laboratory. I acknowledge thanks to all the members of Zollo's group, for their support and for sharing the additional data insert in this PhD thesis to make a more comprehensive thesis work.

My thank extend to Prof. Kris Gevaert, Vlaams Instituut voor Biotechnologie (VIB), Ghent, and to all the members of his laboratory, in particular Jonathan Vandenbussche, An Staes and Kathleen Moens, for helping us in the production and analysis of proteomic data. I would also like to thank Prof. Lennart Martens for the support given for statistical analysis.

Finally, my gratefulness goes to my family, which allowed my dream became true.